Circulation Statistics Derived from Level III-b and Station-Based Analyses during FGGE

RICHARD D. ROSEN AND DAVID A. SALSTEIN

Atmospheric and Environmental Research, Inc., Cambridge, MA 02139

JOSÉ P. PEIXOTO

Geophysical Institute, University of Lisbon, Lisbon, Portugal

ABRAHAM H. OORT AND NGAR-CHEUNG LAU

Geophysical Fluid Dynamics Laboratory/NOAA, Princeton University, Princeton, NJ 08542

(Manuscript received 10 March 1984, in final form 10 October 1984)

ABSTRACT

A number of Northern Hemisphere circulation fields and statistics are derived for the months of January and June 1979 from level III-b analyses produced by GFDL using a 4-dimensional data assimilation scheme which incorporates measurements from a wide variety of sources. In particular, hemispheric maps and zonal cross sections of the wind, specific humidity, and the eddy fluxes of momentum, heat and moisture are examined. Certain quantities related to the atmosphere's energy cycle are also considered. These fields and statistics are compared with those derived from analyses that rely solely on the conventional rawinsonde station data taken during the same months. In the case of the monthly mean zonal and meridional winds, we also present results based on the level III-b analyses of the ECMWF.

The station-based analyses yield zonal mean statistics and hemispheric integrals that are generally comparable to those from the level III-b analyses. For example, the intensity of the Northern Hemisphere Hadley cell in January produced by the station analyses lies between those of the III-b analyses, which differ by as much as 35%. On regional scales, however, there are some large differences in the circulation fields between the station-based and level III-b analyses over areas of sparse station coverage. For example, the station-based analysis of the 200 mb field of transient eddy momentum flux in January does not include a significant region of northward flux over the northeast Pacific that is contained in the GFDL analysis. It is not yet clear, though, to what extent model biases may be affecting the GFDL analysis in this or in other station-sparse areas. In the case of the subtropical Pacific jet in January, the station-based analysis appears to underestimate its extent, but there are also considerable differences between the two level III-b analyses in this region. In addition, the GFDL analyses often appear to be noisy. Improvements in the level III-b analyses need to be made before full confidence can be placed in results based on modern data assimilation techniques.

1. Introduction

The traditional source of atmospheric circulation statistics has been the set of observations collected at the network of upper-air sounding stations. A comprehensive collection of such station-based statistics has recently been published by Oort (1983), for example. Gaps in the spatial distribution of the stations, particularly over the oceans, raise inevitable questions, however, about the accuracy of such statistics. Oort (1978) addressed these questions with the aid of numerical model simulations, but further examination of the issue is certainly warranted.

The extensive data set gathered by the First GARP Global Experiment (FGGE) offers an opportunity for such a further examination. Extraordinary efforts were made during the FGGE to fill the rawinsonde station-void regions of the globe with observations from a variety of other platforms, including aircraft, ships and satellites. The resulting assortment of measurements has been combined using numerical forecast/assimilation models to generate so-called level III-b global grid point analyses of the atmosphere for the FGGE year. An important question is whether circulation statistics derived from these level III-b analyses reveal important features that have been missed by the station network during FGGE and possibly, therefore, in earlier years as well. Or do the level III-b statistics provide a view of the general circulation that is reasonably similar to that given by the rawinsonde stations alone? Answers to these questions are an important goal of the work reported here.

Because the techniques used to generate grid point analyses like the level III-b analyses involve blending observations with an initial guess provided by a

forecast model, biases in the model or other elements of the assimilation scheme can affect circulation statistics derived from these analyses. An extreme example of this, shown by Rosen and Salstein (1980), is the complete absence of mean meridional cells from an early version of the National Meteorological Center (NMC) analysis. With regard to the FGGE level III-b analyses, Kung and Tanaka (1983) have already discovered that the intensity of the energy cycle is quite sensitive to the data assimilation used. Another goal of our research, therefore, is to help assess the effects of the FGGE data assimilation schemes on large-scale circulation statistics. This assessment may, in turn, yield insights into means for further improving existing data assimilation approaches.

Level III-b analyses for the entire FGGE year have been made at the Geophysical Fluid Dynamics Laboratory (GFDL) of the U.S. National Oceanic and Atmospheric Administration, and at the European Centre for Medium Range Weather Forecasts (ECMWF). Because a number of diagnostic calculations based on the ECMWF analyses are already available (for example, Kanamitsu, 1981; Bengtsson *et al.*, 1982b; Bengtsson, 1983; Lorenc and Swinbank, 1984), we focus here on circulation statistics derived from the GFDL analyses and on comparisons of the GFDL statistics with those derived from FGGE rawinsonde data. In this respect, the current study resembles those by Rosen and Salstein (1980) and Lau and Oort (1981, 1982), in which statistics derived from NMC analyses were contrasted with those from contemporaneous rawinsonde data in order to assess the merits and weaknesses of each. As in these earlier papers, we consider circulation statistics derived in what Oort (1964) labeled the mixed space–time domain, thereby separating eddy quantities into their traditional standing and transient components.

In some instances, results from the ECMWF level III-b analyses are also included here to compare the impact of two different assimilation schemes. Given the complexities involved in generating level III-b analyses, it may not always be possible to identify the cause for differences that emerge between the two III-b analyses. Even so, it remains important simply to document that such differences exist, because they serve as a measure of the uncertainty in using the FGGE data to define the general circulation. Moreover, because both the GFDL and ECMWF level III-b analyses are being used widely in a variety of studies, a general appreciation for the nature of the differences between them is highly desirable.

Results are presented here for only two individual months of the FGGE year, January and June 1979. Both months were part of FGGE Special Observing Periods (SOPs), during which intensive data sets were collected and special *in situ* platforms, such as the tropical wind observing ships, were deployed. The better data coverage during these two months warrants the restriction to them here, although some of our conclusions must, of course, be tempered by the shortness of these samples. Also, our purpose here is not to present a complete compendium of circulation statistics. An atlas containing an extensive set of such statistics for the entire FGGE year based on the GFDL analyses, and including comparisons with the ECMWF analyses for the SOPs, has been prepared by Lau (1984a,b).

2. Data and analysis

a. Upper-air station data

Although station-based climatologies of circulation statistics do exist against which we can compare the FGGE level III-b statistics, the degree of interannual variability in monthly mean circulation fields is large enough to question the usefulness of such an approach. We, therefore, chose to work with the rawinsonde data collected during the FGGE itself to create station-based statistics.

All observations from the fixed upper-air stations and the tropical wind observing ships (TWOS) for 0000 GMT were acquired for the months of January and June 1979 from the Main Level II-b data set archived at the World Data Center-A (Asheville). These observations were screened for gross errors, inconsistent station locations and duplicate reports. Then means, variances and covariances of the quantities u, v, T and q (zonal wind, meridional wind, temperature and specific humidity, respectively) were formed at each standard level (surface, 1000, 850, 700, 500, 400, 300, 250, 200, 150, 100, 70 and 50 mb) of each station, separately for each of the two months. For stations north of 30°N, levels that contained fewer than 15 observations for the month were dropped from further analysis; the cutoff criterion was lowered to 10 observations for tropical stations, although the bulk of the tropical stations did pass the stricter criterion. In addition, monthly station values at a given level that departed from the average of all the stations by more than 3 standard deviations were subjected to further scrutiny, which in a few cases resulted in their being dropped.

Rawinsonde information was available during the SOPs not only from the fixed station network but also from the TWOS, which in many cases were maintained at fixed or nearly fixed sites. In these cases, daily values were included in the monthly mean, variance and covariance statistics only when the ship lay within a certain radius of its monthly mean position (generally about 250 km). In all other respects, the data from the TWOS were handled in the same manner as those from the fixed upper-air stations.

Despite the extensive efforts made for the FGGE, the rawinsonde coverage south of about 20°S re-

mained inadequate that year for analyses of the Southern Hemisphere (SH) based on these data alone. Therefore, results are presented for the Northern Hemisphere (NH) only, which, however, do make use of the tropical Southern Hemisphere data to guide the analysis in the equatorial region. Table 1 contains the number of stations north of 20°S that passed the cutoff criterion at each level for January and June. Included in the table are statistics for 950 and 900 mb, despite the lack of directly observed winds at these two non-standard levels. Monthly mean winds at these two levels were obtained by interpolating between 850 mb and the closer of the surface or 1000 mb, when possible. This had the desirable effect of incorporating some surface level information into our analysis.

A comparison between Table 1 and a similar table for the winter of 1976/77 given by Rosen and Salstein (1980) indicates a slight, but definite, increase in the number of stations reporting during the FGGE. The most important factor influencing the quality of the station-based analyses, of course, is the spatial distribution of the stations. Figure 1 contains hemispheric maps of the stations that passed the cutoff criterion at the 850 and 200 mb levels for January and June 1979. The most significant differences in station distribution between the two months are the shift in location of an array of TWOS within the Indian Ocean, and somewhat lesser coverage in January over eastern Africa and the northern coast of South America. Overall, the distribution of upper-air stations during the SOPs resembles that of other recent years, with a preponderance of stations located over the land in mid-latitudes and large data voids over certain oceanic areas. Some of these voids were at one time filled by the ocean weather ships.

Important improvements in the station network during FGGE are also evident, however, particularly in the equatorial Atlantic with the inclusion of the TWOS and in South America and Africa. Many of the upper-air measurements over Africa were actually made with pilot balloons and not rawinsondes and hence provide low-level wind data only. The coverage in the tropical west Pacific and in portions of the Indian Ocean has also been improved somewhat.

Having formed monthly mean statistics at each station, the next task was to translate this information onto a regular array of grid points. The approach for doing so utilizes objective analysis algorithms described in some detail by Oort and Rasmusson (1971) and Rosen *et al.* (1979). Essentially, the analysis scheme consists of prescribing an initial guess field independently for each quantity over an array of points which project onto a polar stereographic map of the globe from the North Pole to about 20°S. In data-rich regions, the initial guess is modified simply by interpolating corrections based on the station values of the quantity to the surrounding grid points. In data-sparse regions, the analyzed field is mathematically constrained to maintain the same shape (i.e., the same Laplacian) as the initial guess field there. Finally, smoothing operators are employed and steps are taken to ensure that the analysis does not generate unreasonable values of horizontal wind divergence.

Although the initial guess has little impact in the data-rich areas, it does exert a strong influence in data-sparse regions. Because large portions of the hemisphere do not contain upper-air stations, the influence of the initial guess can be seen even in zonal mean statistics. To provide a measure of this uncertainty in some of the station-based statistics, we will present a few results based on different choices of initial guess.

TABLE 1. Number of stations used to construct the station-based horizontal wind analyses at each level for January and, in italic, June 1979.

Level (mb)	Total number of stations	Distribution of stations by latitude belt			
		20°S–Equator	Equator–30°N	30°–60°N	60°N–pole
1000	411 (*364*)	23 (*23*)	128 (*109*)	185 (*160*)	75 (*72*)
950*	564 (*555*)	31 (*31*)	148 (*148*)	298 (*285*)	87 (*91*)
900*	620 (*611*)	32 (*32*)	153 (155)	347 (*331*)	88 (*93*)
850	898 (*891*)	96 (*88*)	262 (*275*)	449 (*434*)	91 (*94*)
700	851 (*869*)	69 (*73*)	247 (*258*)	445 (*439*)	90 (*99*)
500	747 (*758*)	60 (*56*)	196 (*195*)	402 (*410*)	89 (*97*)
400	721 (*732*)	58 (*53*)	186 (*188*)	389 (*392*)	88 (*99*)
300	701 (*728*)	58 (*53*)	180 (*187*)	376 (*390*)	87 (*98*)
250	696 (*714*)	55 (*52*)	178 (*183*)	374 (*383*)	89 (*96*)
200	681 (*713*)	53 (*53*)	171 (*180*)	369 (*384*)	88 (*96*)
150	649 (*692*)	47 (*50*)	160 (*172*)	354 (*374*)	88 (*96*)
100	610 (*653*)	43 (*44*)	144 (*161*)	339 (*355*)	84 (*93*)
70	512 (*566*)	26 (*31*)	126 (*138*)	286 (*310*)	74 (*87*)
50	455 (*532*)	19 (*22*)	118 (*124*)	261 (*302*)	57 (*84*)

* Data obtained from interpolation of values at 850 mb and at either surface or 1000 mb.

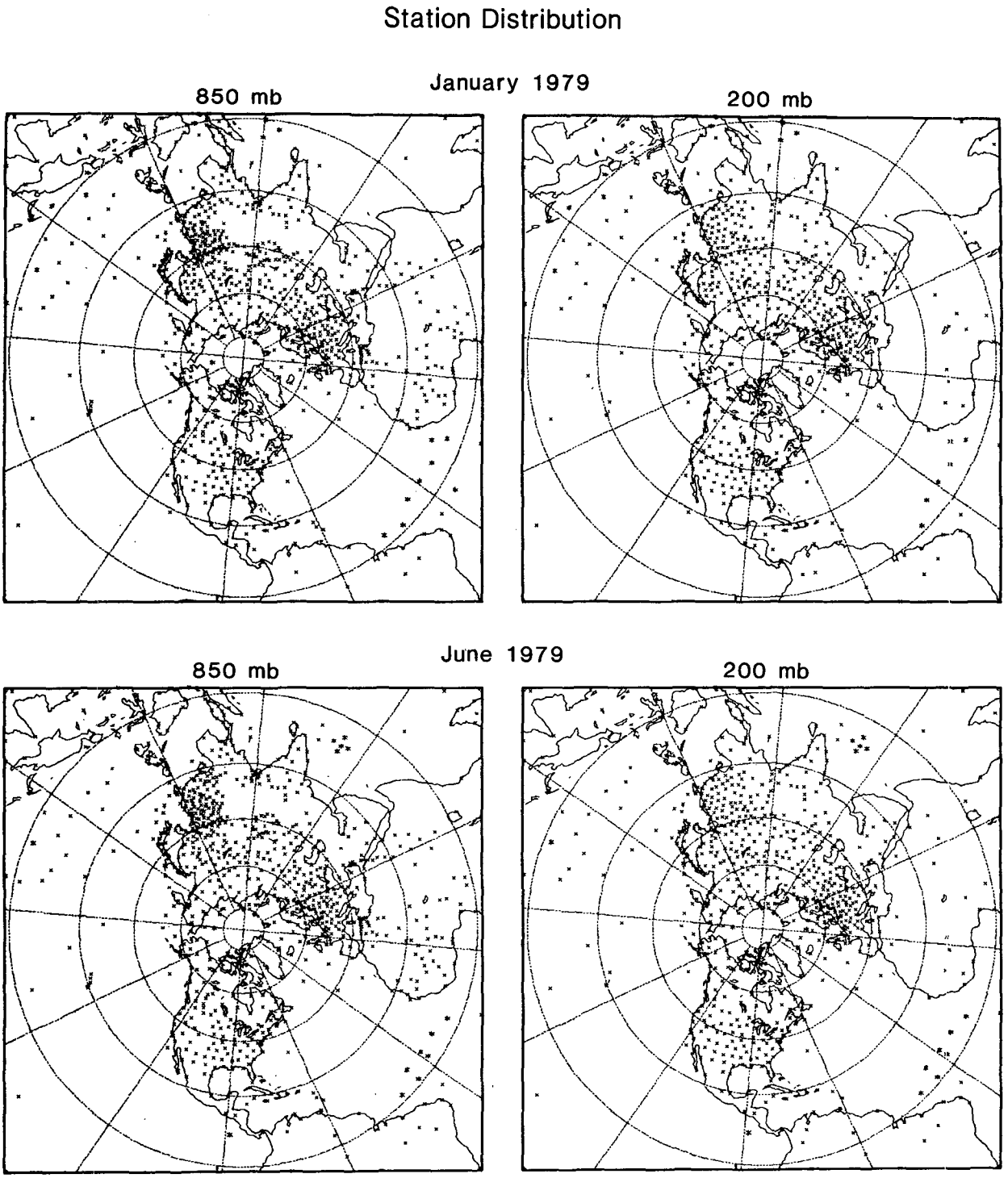

FIG. 1. Maps of rawinsonde stations that passed cutoff criterion for winds at 850 and 200 mb during January and June 1979. Asterisks denote monthly mean location of tropical wind observing ships (TWOS) used in our analysis.

b. Level III-b data

The desire to utilize measurements from the wide host of observing platforms available during the FGGE helped stimulate the development of sophisticated data assimilation techniques at both GFDL and ECMWF. Although both centers have global circulation models at the heart of their data assimilation

systems, their approaches are otherwise quite distinct. At GFDL, data are pre-processed with the aid of a univariate optimum interpolation scheme and then inserted into a global spectral transform model at each model time step (approximately 15 minutes). A nonlinear normal mode initialization is applied every six hours to control the amplitude of high-frequency noise, but it is not allowed to affect slower gravity modes, such as those associated with the tropical Hadley cell. Further details are given by Gordon and Stern (1982) and Stern and Ploshay (1983).

On the other hand, at ECMWF a global grid point model is used to generate a 6-hour forecast, which then is updated with data at verification time using a multivariate optimum interpolation scheme. The multivariate approach utilized by ECMWF imposes a geostrophic constraint on the analyzed corrections to the first-guess field. The ECMWF also applies a nonlinear normal mode initialization, but in its case no explicit attempt is made to maintain modes relevant to the tropical Hadley cell. Further details about the ECMWF analyses are provided by Bengtsson *et al.* (1982a).

In addition to the aforementioned points, other important differences between the GFDL and ECMWF data assimilation systems exist in the data quality control procedures, in the number of observations allowed to affect the analysis at a grid point, and in the weights assigned to different observing platforms during optimum interpolation. Moreover, the global circulation models used by each center employ somewhat different physics. For example, a diurnal cycle was included in the radiation physics of the GFDL model but not in the ECMWF. It is reasonable to expect that the cumulative result of these differences would be to yield different GFDL and ECMWF level III-b analyses, but, without the sort of comparison being presented here, it is difficult to assess *a priori* the magnitude of this difference.

Grid point values from the GFDL analyses were obtained at every 1.875° in latitude and longitude and at the pressure levels of 1000, 950, 900, 850, 700, 500, 300, 200, 150, 100, 50 and 10 mb. The ECMWF analyses used here had the same horizontal resolution but were at the pressure levels of 1000, 850, 700, 500, 300, 200, 150, 100 and 50 mb. The level III-b grid point data were processed next in the same manner as the station data, by forming monthly means and cross-products of the various meteorological quantities at each grid point and level. Finally, two differences between our station statistics and those derived from the III-b analyses should be mentioned. First, we used both 0000 and 1200 GMT level III-b analyses, but only once-daily station data. Based on comparisons between monthly mean statistics derived from once- and twice-daily GFDL level III-b analyses, however, we have found that this difference does not significantly affect the quantities considered here. Second, unlike the case for the individual stations, there are no missing days in the level III-b data.

3. Mean wind fields

A fundamental test of our ability to measure the general circulation can be made by assessing the accuracy of the monthly mean fields of the basic wind components, u and v. For this reason, special attention is devoted to these fields here and a more extensive set of comparisons is presented for them. In particular, we will present the monthly mean u and v fields from two different versions of the station-based analysis as well as from the GFDL and ECMWF level III-b analyses.

As noted earlier, results from the station analyses are dependent on the initial guess field. This sensitivity is shown here with the aid of two different initial guess procedures that have been used in the past. In the first version, called the "climatology/vertical continuity" approach, the initial guess for the 1000 mb level is taken from a long-term collection of hemispheric data assembled in atlas form by the U.S. Navy (1966), supplemented by data from selected tropical pilot balloon stations. Above 1000 mb, the initial guess field is the nondivergent part of the final analyzed field at the level immediately below. In the second version, called the "zonal initial guess" approach, the zonal mean of all station values within each latitude belt is formed, independently at each level. In this second case, latitude belts were generally chosen to be 10° wide. The initial guess was formed by assigning to each grid point in a belt the appropriate zonal mean and then smoothing this field to minimize discontinuities between neighboring zones.

Previous comparisons (Starr *et al.*, 1970) have found that zonal means tend to be larger when the zonal initial guess approach is used. In the case of the zonal wind, differences in the zonal means in the vicinity of the jet are typically about 10%. Relative differences in the zonal means of the meridional wind can be much larger than this, however.

a. Monthly mean zonal wind, $\bar{u}$

Figure 2 contains cross-sections of $[\bar{u}]$ (the brackets denote a zonal mean and the overbar a monthly mean) for January and June 1979 derived from the two versions of station analysis and the GFDL level III-b data. As in previous studies, the two station versions differ by about 10% near the jet, the larger values being associated with the zonal initial guess version. The strength of the jet in the GFDL analysis is closer to that in the zonal initial guess station analysis in January, but closer to that in the other version of station analysis in June. Despite these differences, it is clear that the analyses of $[\bar{u}]$ are, in general, in good agreement.

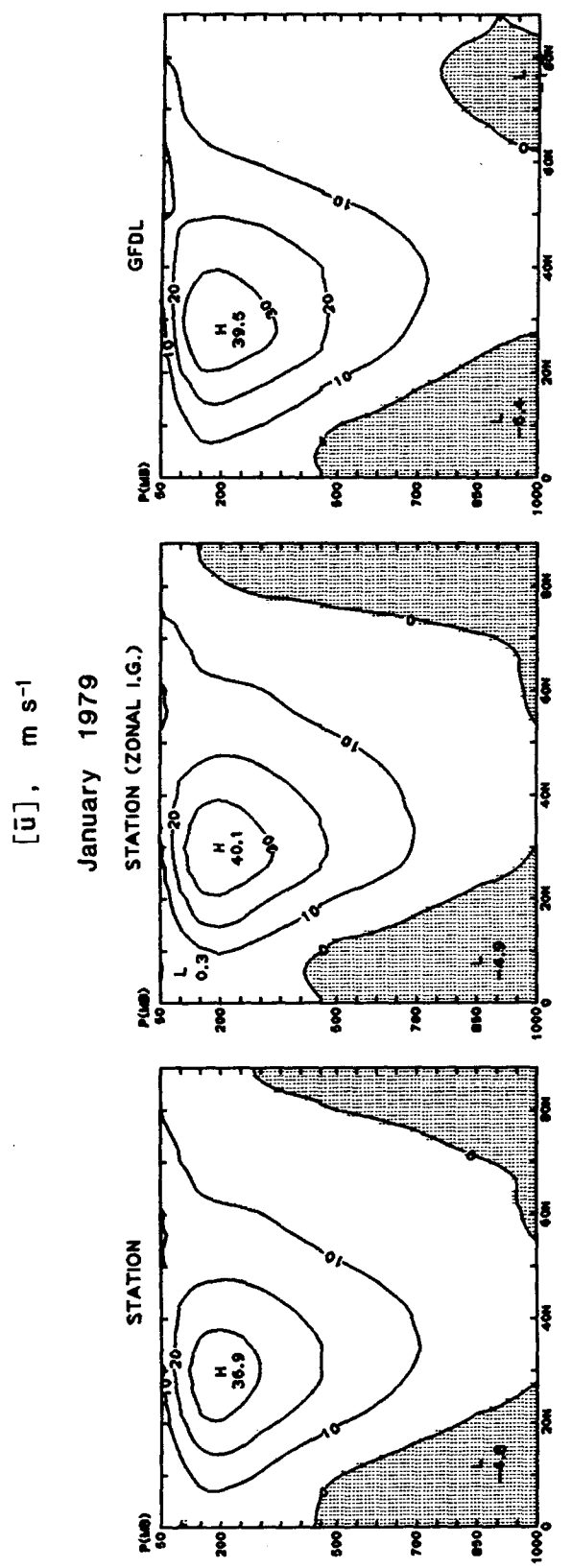

FIG. 2. Cross sections of the zonally averaged mean zonal wind for January and June 1979 based on two versions of station analysis ("climatology/vertical continuity" and "zonal initial guess") and the GFDL level III-b analysis. Negative values are shaded and indicate easterlies. Locations of extrema in these fields (and all others displayed in the paper) are indicated by the symbols "H" or "L".

Insight into the cause of the differences that do exist among the $[\bar{u}]$ fields may be gained from studying the 200 mb maps of $\bar{u}$ in Fig. 3. Focusing first on the January maps, there is a notable difference between the GFDL and station analyses in the structure of the subtropical jet east of Japan, where the 45 m s^{-1} isoline extends farther eastward over the Pacific in the GFDL analysis than in either of the station analyses.

Of the two station analyses, the zonal initial guess version tends to yield the stronger zonal pattern, as evidenced by the more nearly continuous subtropical belt of winds greater than 30 m s^{-1} in this version. Interestingly, the only break in this belt occurs over the station-void Arabian Sea (where an even stronger minimum exists in the other station analysis version), whereas the GFDL analysis contains an unbroken area of winds greater than 30 m s^{-1} in this region. On the other hand, over the station-sparse subtropical Atlantic, there is a notable break in the area of greater than 30 m s^{-1} winds in the GFDL analysis, but not in either station analysis.

As an aside, we should comment on the isolated maximum in $\bar{u}$ that appears north of Hawaii in the zonal initial guess version of the station analysis, but not in either of the other two analyses. This maximum is an artifact of the zonal initial guess procedure used here, and does not reflect real station values. It results from the presence of a strong meridional gradient in the initial guess field that is maintained by the final analysis in this data-sparse area.

Turning to the 200 mb maps of $\bar{u}$ for June in Fig. 3b, there are two differences between the level III-b analysis and the station analyses worth noting. The first is located in the central Pacific, north of Hawaii. Here the III-b analysis depicts a large tongue of weak westerlies, whose extent is greatly underestimated by both station analyses. The second region of widespread difference is over northwest Africa and the adjacent Atlantic, where the III-b analysis depicts a continuous band of westerlies greater than 15 m s^{-1}. In both station analyses, however, winds this strong do not extend west of 10°E over Africa. Referring back to the station maps of Fig. 1, we see that this region contains very few conventional data at 200 mb, because it is well above the level that the pilot balloons used in Africa report. The quality of the station analyses must, therefore, be regarded as suspect here.

The differences between the GFDL and station analyses cited above are mainly confined to the station-sparse regions of the hemisphere. It would seem reasonable, therefore, that the GFDL analyses would better represent the actual $\bar{u}$ fields in these regions, where they often had the benefit of additional, nonconventional data. However, it is interesting to compare the GFDL analysis with that of the ECMWF, which also used the full set of FGGE observations, as shown in Fig. 4 for the January $\bar{u}$ field at 200 mb. Although the GFDL and ECMWF analyses generally agree quite well, there are two areas in Fig. 4b in which differences as large as 10 m s^{-1} occur. The first of these is located in the exit region of the east Asian jet over the Pacific, an area already noted above in connection with the station analyses. The second area of large differences in Fig. 4b is over central Asia.

These two areas are highlighted in the maps in Fig. 5 for the strip 150–300°W and 20–40°N. Superimposed on the analyses are the available station values of $\bar{u}$ for January at 200 mb. The reason for the relatively weak jet in the zonal winds over the Pacific in the station analyses of Fig. 3a is now evident: station 91066 (Midway at 28.2°N, 177.4°W), whose value of 32 m s^{-1} is based on 26 daily observations during the month, exerts a controlling influence on the station analyses in this region. Apparently the level III-b analyses were more strongly influenced by satellite and aircraft data available in this region. It is clear, though, that there are important differences in how these data are assimilated into the two level III-b analyses.

Over India, the picture is somewhat confused by the disparity in station values near 278°W. One station there reports a monthly mean of 55 m s^{-1} (based on 22 observations), whereas its neighbor yields a mean of 28 m s^{-1} (based on 13 observations). The ECMWF analysis draws a 45 m s^{-1} isoline around the two stations, but the GFDL analysis produces weaker winds there and to the north of the region. Farther east, in the vicinity of 260°W, there is another maximum in the difference field in Fig. 5. In this case, the ECMWF analysis appears to more closely reflect the data from the dense collection of rawinsonde stations.

Without resort to the nonconventional data included in the level III-b analyses and much further investigation, it is not possible to fully assess the correctness of one level III-b analysis over the other in much of the tropical strip of Fig. 5. In any case, the magnitude of the differences in the III-b analyses of $\bar{u}$ shows the limitations in the ability to properly depict even this fundamental field.

b. Monthly mean meridional wind, $\bar{v}$

As is well known, the zonal mean meridional wind $[\bar{v}]$ is much weaker than $[\bar{u}]$, reaching maxima of only about 3 m s^{-1} in the winter Hadley cell. Around most latitude circles, $[\bar{v}]$ is a small difference arising from regions of contrasting monthly mean northerlies and southerlies. Indeed, $[\bar{v}]$ represents the divergent part of the meridional wind and has therefore been difficult to measure accurately.

Rather than present results for $[\bar{v}]$ directly, we will show here the mass streamfunction ψ, which is related to $[\bar{v}]$ through the equation

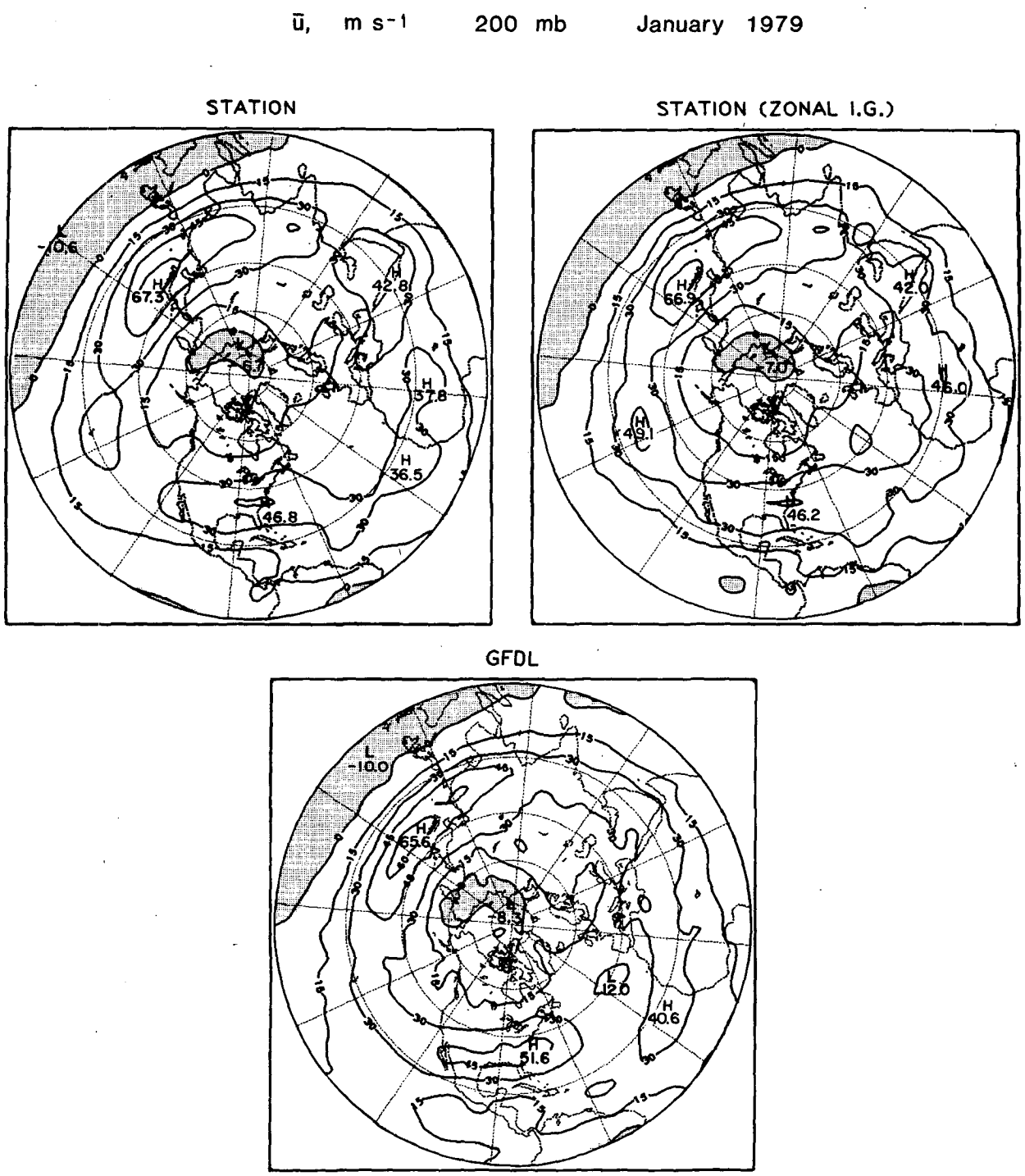

FIG. 3a Hemispheric maps of the mean zonal velocity at 200 mb for January 1979. Results are derived from the two versions of station analysis and the GFDL level III-b analysis. Isolines are drawn at intervals of 15 m s^{-1}. Negative values are shaded and indicate easterlies.

$$\frac{\partial \psi}{\partial p} = 2\pi a \cos\phi \, g^{-1}[\bar{v}],$$

where p is pressure, ϕ latitude, a mean radius of the earth and g acceleration due to gravity. Before computing the streamfunction, it is necessary to subtract from $[\bar{v}]$ any spurious net flows of mass across latitude walls. Such mass flows have long been a feature of station-based analyses (Rosen, 1976), but it is disappointing to note that they are still present

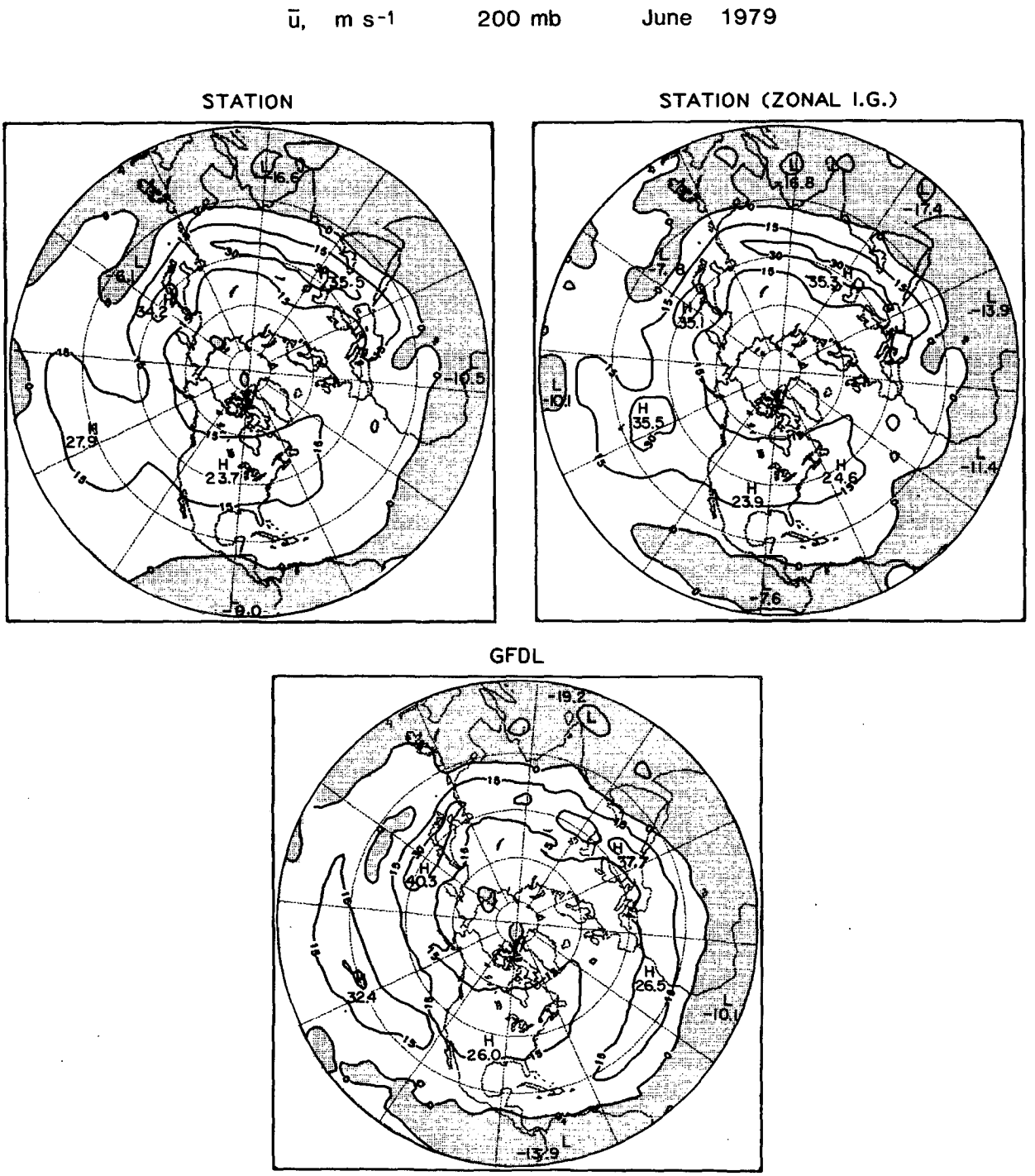

FIG. 3b. As in Fig. 3a, but for June 1979.

in the FGGE level III-b analyses. Indeed, many of the GFDL values for this flux are larger than those in the station analyses (not shown). In January, the GFDL value for the mass flux across the equator would imply an average increase in surface pressure over the NH of about 100 mb! On a more sanguine note, however, the size of the correction for the spurious mass flow to the maximum value of $[\bar{v}]$ in the GFDL level III-b January analysis is only on the order of 10%.

To correct for the spurious mass flow at each latitude, we simply subtracted the vertical mean of

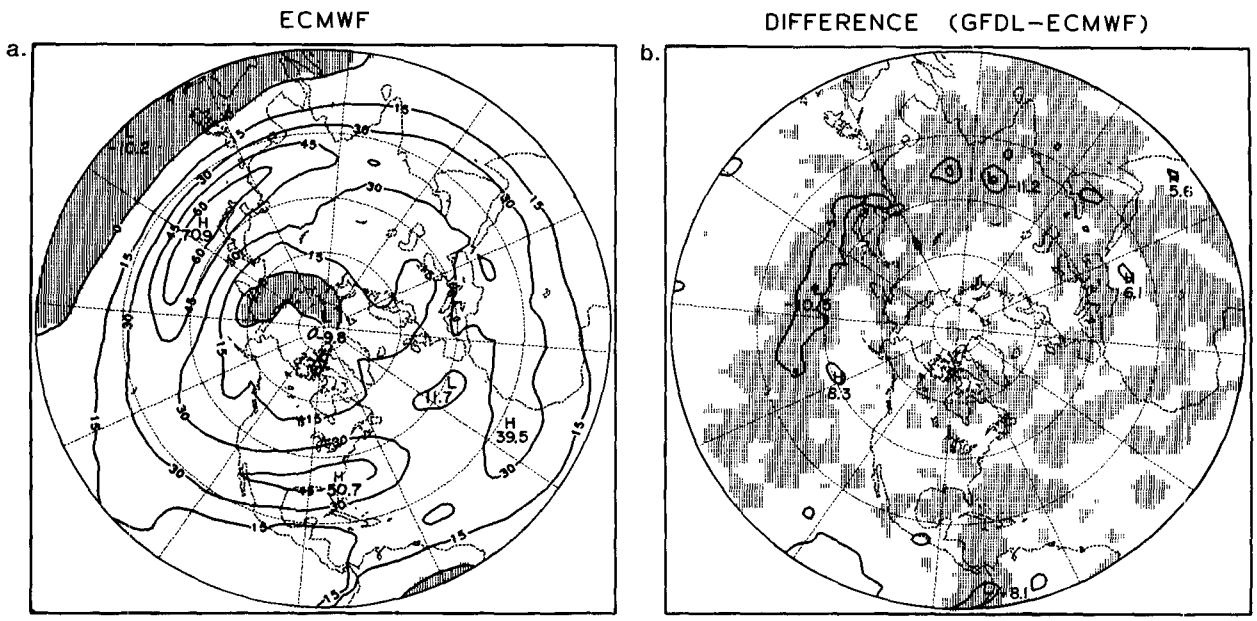

FIG. 4. (a) Hemispheric map of the mean zonal velocity at 200 mb for January 1979 based on the ECMWF level III-b analysis. Isolines are drawn at intervals of 15 m s^{-1}. Negative values are shaded and indicate easterlies. (b) Hemispheric map of the GFDL field in Fig. 3a minus the ECMWF field in Fig. 4a. Isolines are drawn at intervals of 5 m s^{-1} (the zero line is omitted). Negative values are shaded and indicate regions of stronger westerlies or weaker easterlies in the ECMWF data.

$[\bar{v}]$ from the individual values at every pressure level. These normalized $[\bar{v}]$ values were then used in the above equation (after setting $\psi = 0$ at 50 mb) to generate the streamfunction fields in Fig. 6. In Fig. 6a for January, the maximum values in the Hadley cell of the two station versions are within 20% of each other. This correspondence between the two station approaches is much better than in previous studies and reflects the improvement in the tropical station coverage during the SOPs. The GFDL III-b mass streamfunction for January appears to be quite realistic, differing from the station analyses in only two respects. First, the vertical gradient of ψ in the lower levels of the tropics is stronger in the GFDL analysis, leading to a maximum value of ψ in the Hadley cell that is 20% larger than the average of the two station maxima. Second, this central value of ψ is located 200 mb closer to the surface in the GFDL analysis than in the station analyses. These differences are related to a more intense region of tropical low level northerlies, which is confined more strictly to the lower half of the atmosphere, in the GFDL analysis. In the ECMWF streamfunction in Fig. 6a, the Hadley cell seems to be too weak, which Lorenc and Swinbank (1984) attribute to the ECMWF initialization scheme. Also, the tropical zonal mean northerlies are confined to a much shallower layer in the ECMWF analysis than in any of the others.

In June, the maximum value of ψ lies in the tropical Southern Hemisphere, but only the northern reaches of the SH Hadley cell are captured by the Northern Hemisphere plots of Fig. 6b. Even so, it is apparent that this cell is considerably stronger in the GFDL analysis than in the others. Again, the two station analyses are in general agreement, although the zonal initial guess version more closely produces the strength of the NH Hadley cell (near 20°N) yielded by the GFDL analysis. The ECMWF analysis again seems to significantly underestimate the strength of this cell. North of about 40°N, where $[\bar{v}]$ is generally small, all the analyses yield fairly similar pictures.

A sense of the difficulty involved in measuring $[\bar{v}]$ may be gained by considering the maps in Fig. 7a, which portrays the field of $\bar{v}$ at 200 mb in June from the "climatology/vertical continuity" version of station analysis and from the GFDL III-b analysis. (The zonal initial guess station analysis is not presented here, because it so closely resembles the other version in Fig. 7a.) The existence of alternating regions of nearly equally intense northerlies and southerlies around a latitude belt is evident in both maps. Indeed, the two maps depict very much the same pattern, although there are several small areas of large differences (Fig. 7b). In general, the GFDL analysis contains both the stronger northerlies and southerlies,

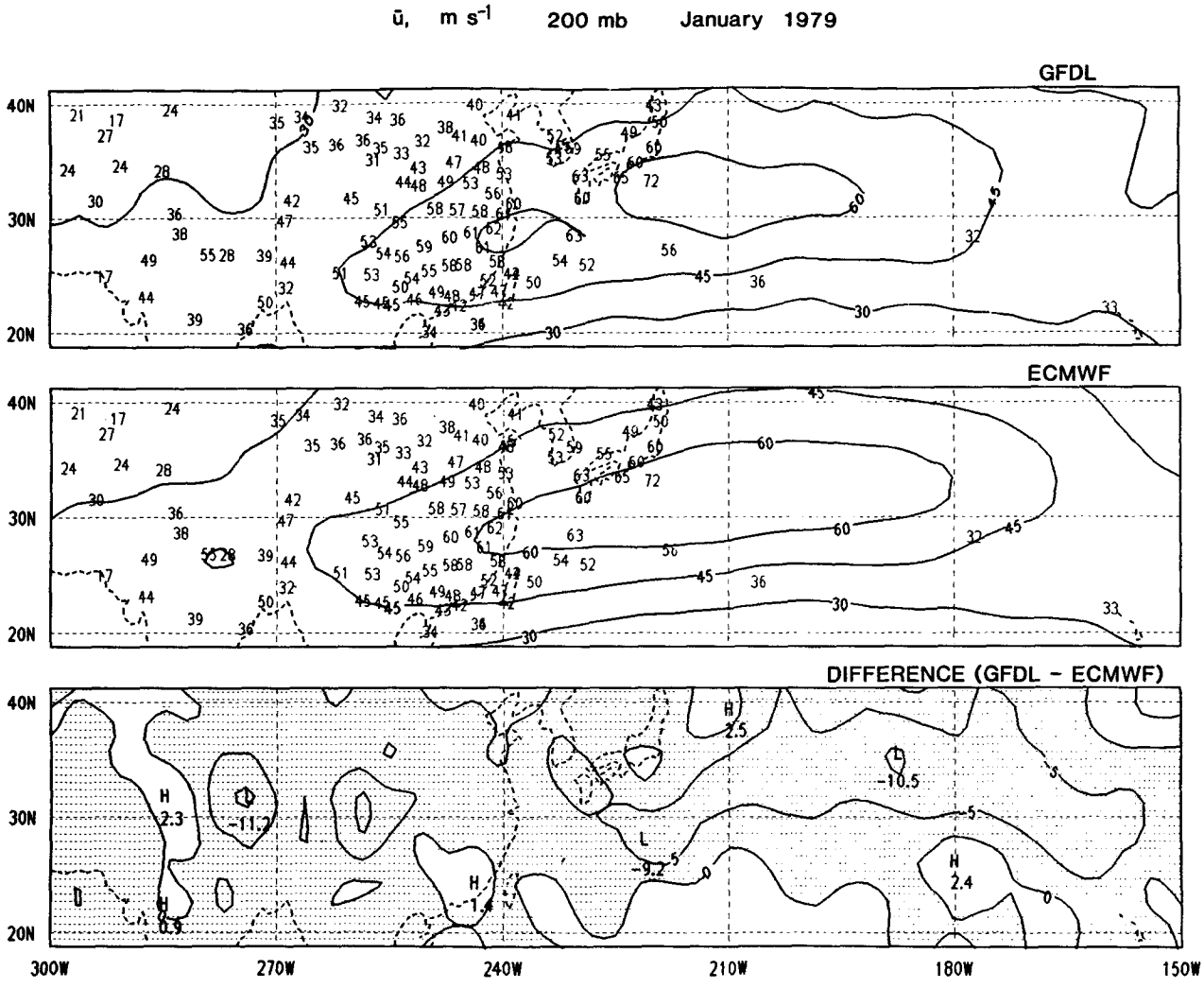

FIG. 5. Map of the zonal velocity at 200 mb for January 1979 in the region from 20 to 40°N and 150 to 300°W calculated from the GFDL (top) and ECMWF (middle) level III-b analyses. Isolines are drawn at intervals of 15 m s^{-1}; also displayed are the monthly mean values of $\bar{u}$ at the rawinsonde stations that passed the cutoff criterion for the month. In the bottom panel is the difference, GFDL minus ECMWF, with isolines drawn at intervals of 5 m s^{-1} and negative values shaded.

so that the differences in Fig. 7b (which are mostly located over gaps in the station network) cancel in the zonal mean, thereby constraining differences in $[\bar{v}]$.

4. Eddy fluxes and energetics

We now turn attention to some second-order moments of the general circulation: in particular, the transient eddy fluxes of momentum and heat and the eddy kinetic and potential energies. For the transient eddy statistics, the initial guess for the station-based analysis is taken to be zero everywhere. The effect of this initial guess is to generate final values in data-sparse regions that are linear interpolations of the values in data-rich regions. In light of the uncertainty involved in knowing how to specify an initial guess for the eddy fields, this seems to be a reasonable approach.

a. Eddy momentum fluxes

Figure 8 contains the January and June zonal mean fields of the transient eddy flux of momentum $[\overline{u'v'}]$, where the prime denotes a deviation from the temporal mean. Both the station and GFDL level III-b analyses yield similar patterns each month, but their intensities do differ markedly. For example, the midlatitude maximum of northward flux is 30% larger in the station analysis in both months. According to Kanamitsu (1981), however, the ECMWF January analysis gives a value for this center that is within about 5% of the present station analysis. Furthermore, the station analysis produces southward

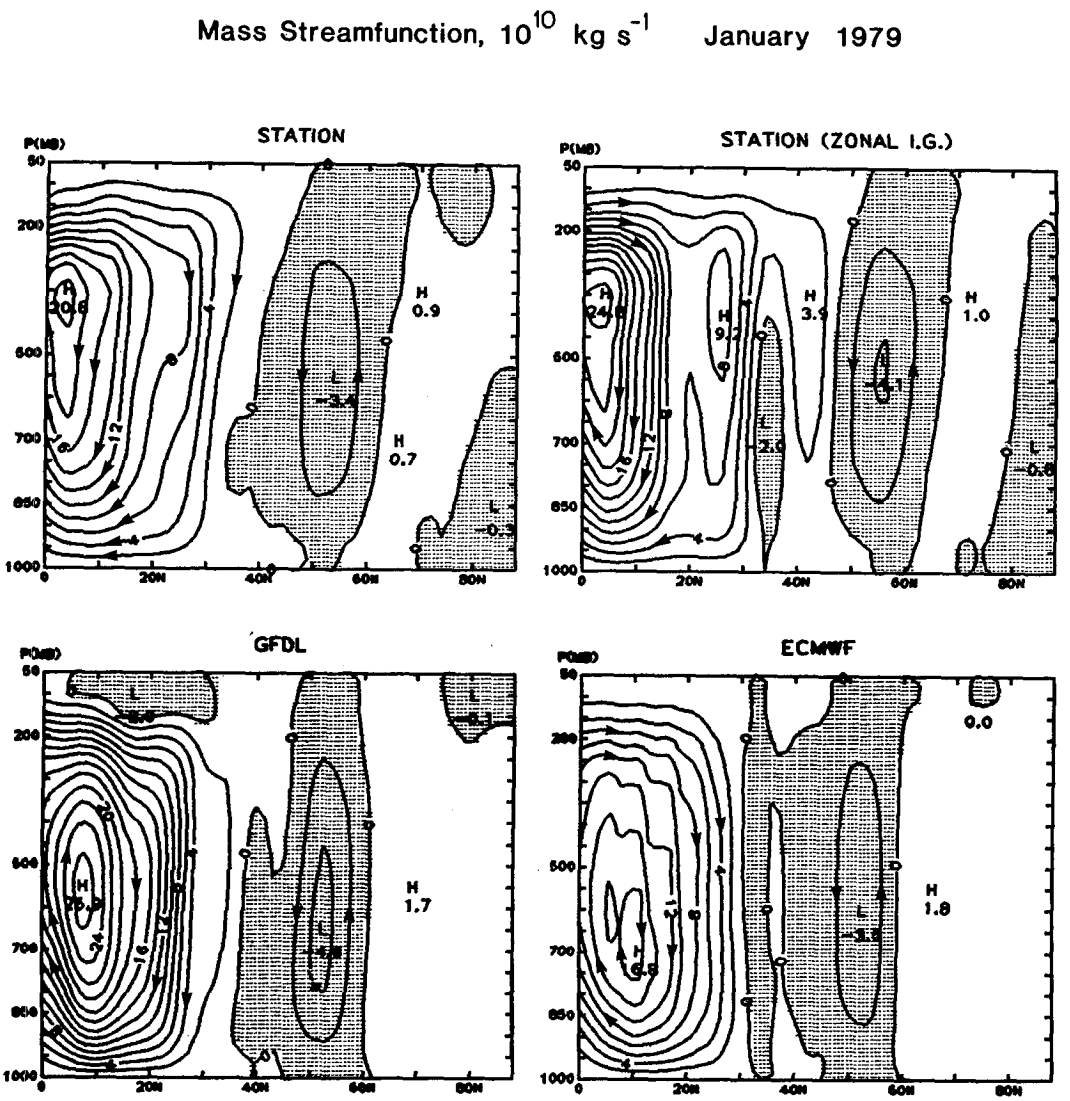

FIG. 6a. Cross sections of the mass streamfunction for the mean meridional circulation obtained after removal of spurious net mass flows for January 1979. Results are presented for both versions of station analysis and for the GFDL and ECMWF level III-b analyses. Positive values indicate clockwise circulation.

fluxes in the tropical upper atmosphere that are much smaller than those in the GFDL analysis in January. However, the comparison by Lorenc and Swinbank (1984) of results for $[\overline{u'v'}]$ from five different FGGE analyses for the region around 5°N indicates that the GFDL value is anomalously strong. In high latitudes, the southward fluxes in the station analysis are considerably stronger in January, but considerably weaker in June.

It is difficult to trace the cause of these zonal mean differences by examining maps of $\overline{u'v'}$, because the local differences in the eddy flux are up to an order of magnitude larger than the zonal means and tend to be of opposite sign around a latitude circle. Nevertheless, it is interesting to inspect maps of $\overline{u'v'}$ from the station and GFDL analyses, as shown in Fig. 9a for the 200 mb level in January. The overall pattern is the same in the two analyses, although the GFDL map is noisier, a point to be returned to later.

The difference map in Fig. 9b contains two areas worthy of special discussion. The first is located in the central north Atlantic, where the once-daily record from station 08509 (Lajes at 38.7°N, 27.1°W) yields an eddy flux greater than 210 m^2 s^{-2}. Most of this flux is associated with a wave that passed over this station during the first five days of January. Indeed, when the eddy flux is recomputed at this site for the period 6–31 January only, the value decreases to 38 m^2 s^{-2}. Clearly, the quantity $\overline{u'v'}$, when calculated for periods as short as a month, can be quite sensitive to

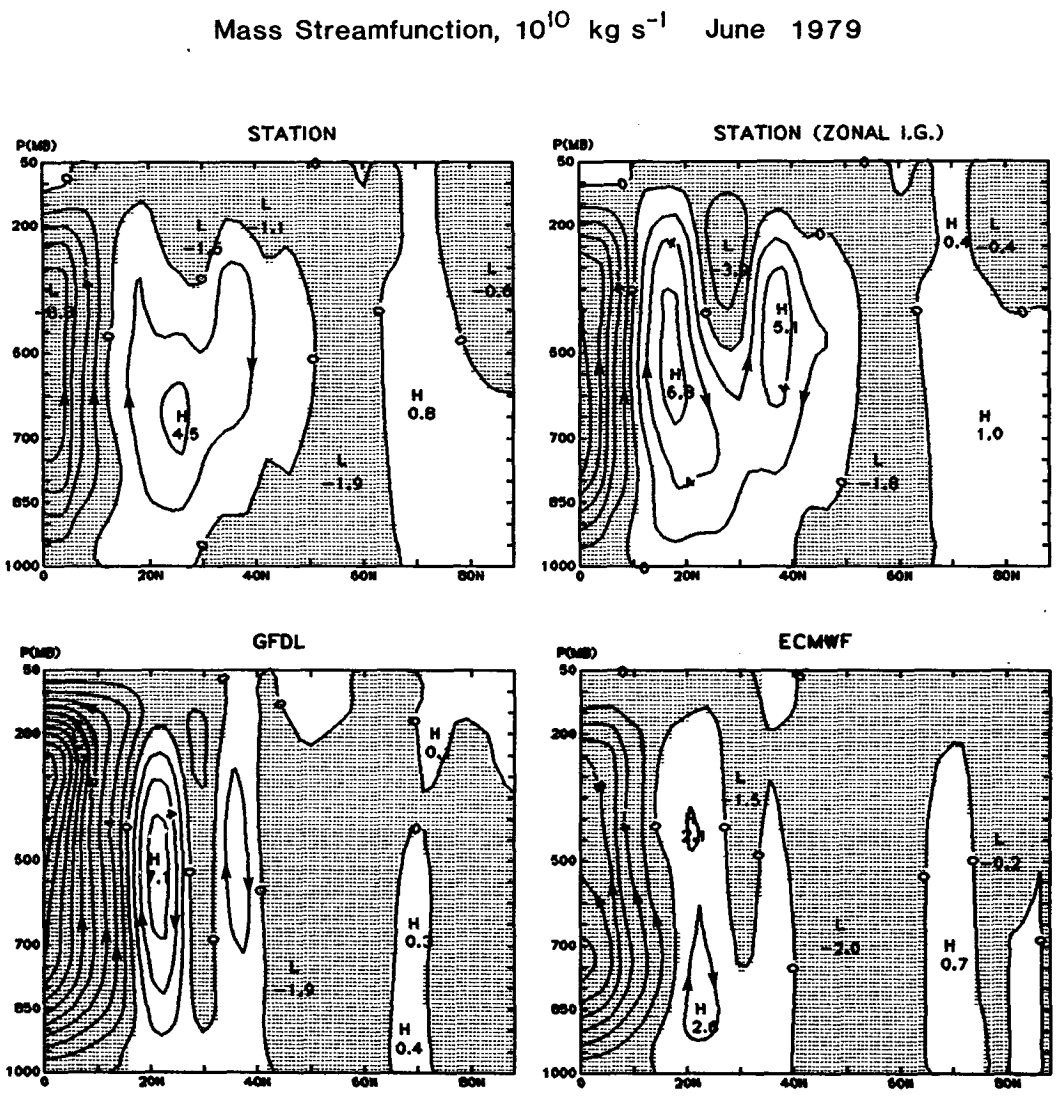

FIG. 6b. As in Fig. 6a, but for June 1979.

the particular choice of monthly interval. This sensitivity does not, of course, affect comparisons between different calculations made for the same month as in Fig. 9. In any case, the GFDL analysis yields a maximum value in this area for the month of January of only about 170 m^2 s^{-2} but more importantly it yields some small, though intense, regions of southward flux around 50°W that are completely missed by the station analysis, which is dominated at this station-void longitude by the value at Lajes. The GFDL analysis also produces a secondary maximum of northward fluxes on the west African coast which lies between the rawinsonde stations in the region.

The second area in Fig. 9b worth highlighting lies in the Pacific between Hawaii and the west coast of the United States. Here the largest value in the GFDL analysis of the NH is to be found, whereas the interpolated values in this station-void region in Fig. 9a are much smaller. Although this feature is of relatively small spatial scale, it is nonetheless quite intense and, if real, points out an important shortcoming in analyses of the momentum flux based only on the current network of stations. On the other hand, it is possible that the GFDL values in this region partly reflect a bias in the GFDL model. Support for this possibility comes from an analysis (not shown) of the climatology of another general circulation model developed at the Goddard Laboratory for Atmospheric Sciences, which contains a strong positive maximum of $\overline{u'v'}$ in this part of the Pacific at 200 mb. Examination of the aircraft and satellite data used in the GFDL analysis in this region would be needed to resolve this point.

On time scales as short as a month, zonal mean momentum fluxes by the stationary eddy component of motion can be comparable to those by the transient

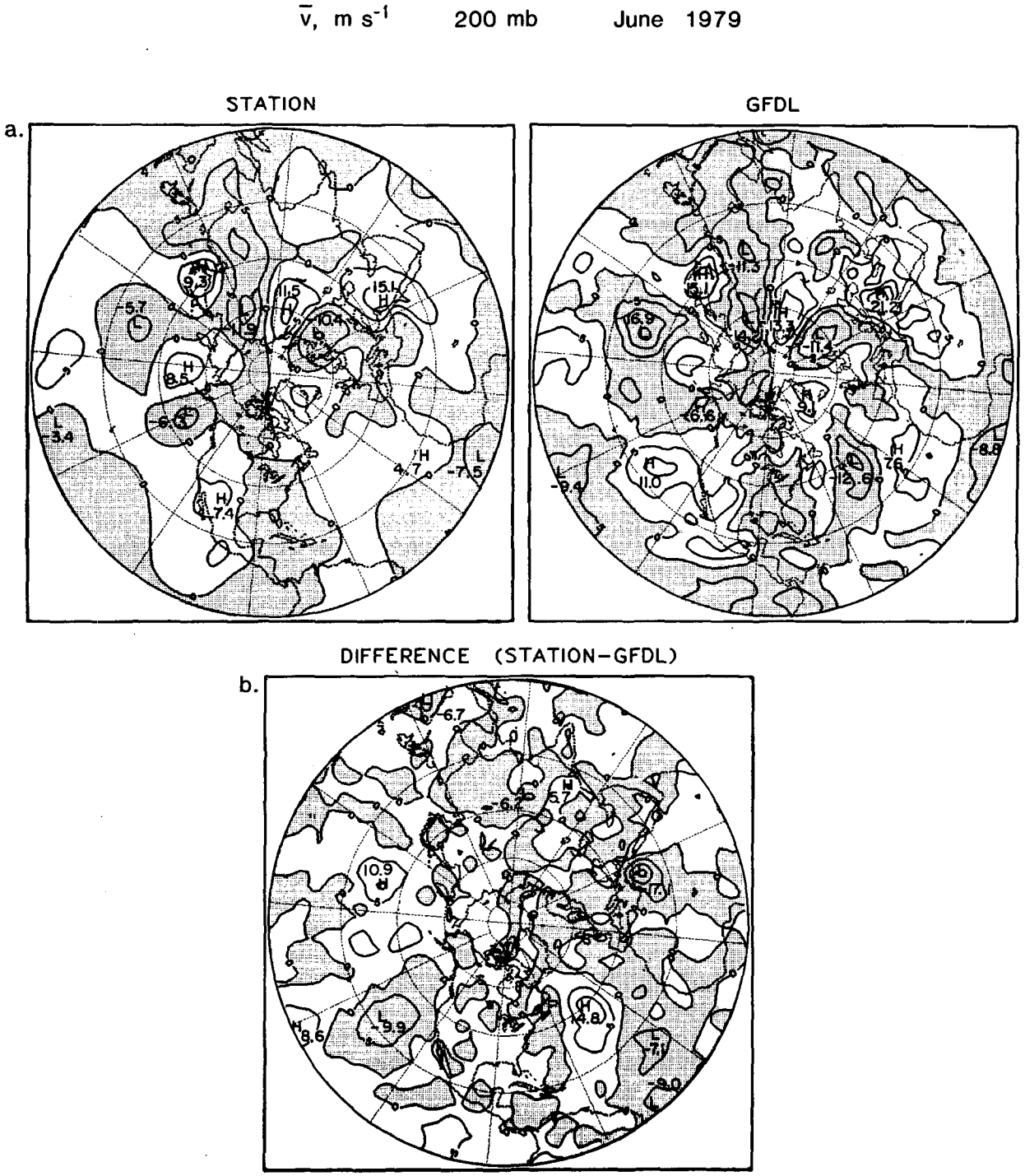

FIG. 7. (a) Hemispheric maps of the mean meridional velocity at 200 mb for June 1979 based on the station and the GFDL level III-b analyses. Isolines are drawn at intervals of 5 m s^{-1}. Negative values are shaded and indicate northerlies. (b) Difference, station analysis minus GFDL analysis, of the two fields in part (a). Isolines are drawn at intervals of 5 m s^{-1}. Negative values are shaded and indicate stronger southerlies or weaker northerlies in the GFDL analysis. (To create the difference values, the GFDL field was interpolated onto the coarser grid used for the station analysis. This same procedure was used to create the difference fields in Figs. 9b and 16b.)

eddies. This was clearly the case for January 1979, as revealed by the plots of $[\bar{u}^*\bar{v}^*]$ in Fig. 10 (the asterisk denotes a deviation from the zonal mean). The figure also shows that the station and GFDL analyses agree fairly well in January. (The station results in Fig. 10 are based on the "climatology/vertical continuity" version of analysis; the zonal initial guess version yields somewhat smaller stationary eddy fluxes.) Both

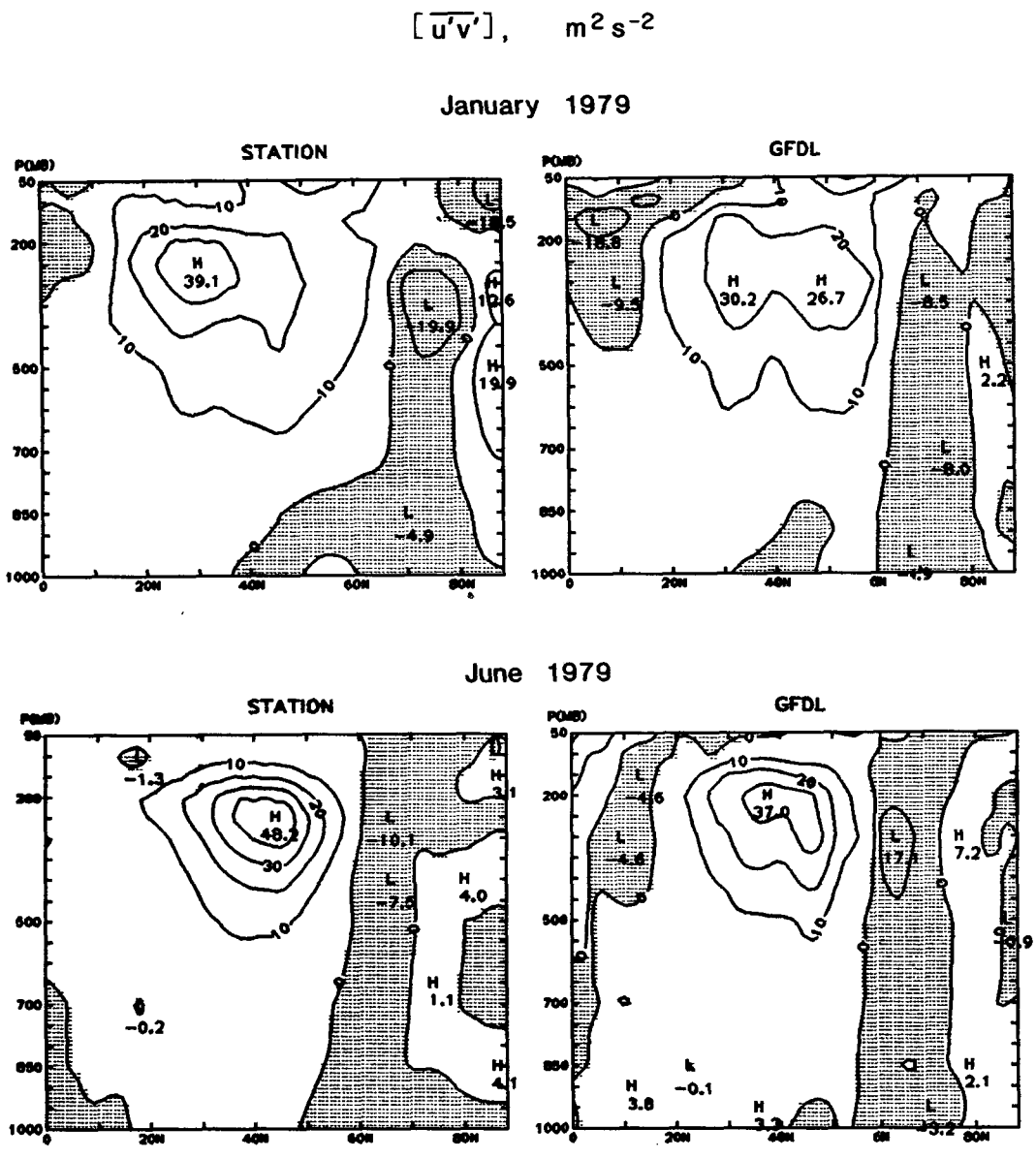

FIG. 8. Cross sections of the transient eddy flux of momentum for January and June 1979 based on the station and the GFDL level III-b analyses. Negative values are shaded and indicate southward fluxes.

analyses, for example, capture the region of strong southward fluxes in the equatorial upper atmosphere that seems to characterize this area in winter (Rosen and Salstein, 1980). In June, the GFDL analysis is dominated by a subtropical maximum in $[\bar{u}^*\bar{v}^*]$ which is nearly twice that contained in the 15-year station-based climatology of Oort (1983). This feature does not appear in the June station analysis which, as noted earlier in connection with Fig. 7, produces a weaker stationary wave pattern in $\bar{v}$ for that month.

b. Eddy heat fluxes

The zonal cross sections in Fig. 11 of the transient eddy flux of heat $[\overline{v'T'}]$ show that closer quantitative agreement exists between the station and GFDL analyses for this quantity than was the case for $[\overline{u'v'}]$. Likewise, the station and GFDL analyses produce comparable results (not shown) for the stationary component $[\bar{v}^*\bar{T}^*]$. The most obvious difference in the transient eddy fluxes in Fig. 11 is perhaps in January in midlatitudes near 300 mb, where the station analysis produces a stronger local minimum in the field.

As in the case for $\overline{u'v'}$, the maps of $\overline{v'T'}$ at 850 mb in Fig. 12 indicate that the GFDL analysis is much noisier than the station-based result. Close inspection of the January $\overline{v'T'}$ field over the station-rich area of North America, for example, reveals a number of small-scale features in the GFDL analysis that are

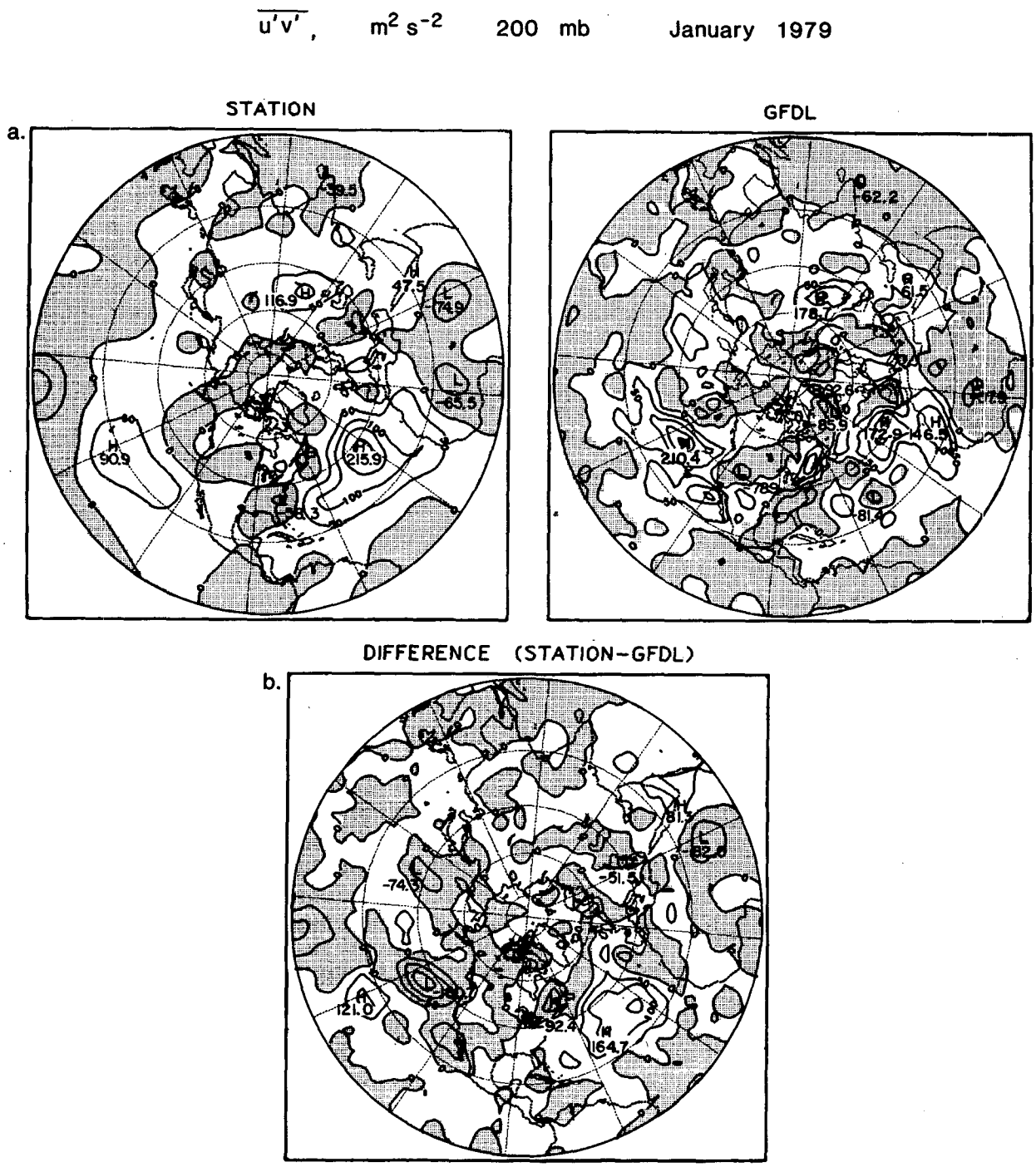

FIG. 9. (a) Hemispheric maps of the transient eddy flux of momentum at 200 mb for January 1979 based on the station and the GFDL level III-b analyses. Isolines are drawn at intervals of 50 $m^2 s^{-2}$. Negative values are shaded and indicate southward fluxes. (b) Difference, station analysis minus GFDL analysis, of the two fields in part a. Isolines are drawn at intervals of 50 $m^2 s^{-2}$. Negative values are shaded and indicate stronger northward or weaker southward fluxes in the GFDL analysis.

not warranted on the basis of the station data. Referring back to the GFDL and ECMWF maps of $\bar{u}$ in Fig. 5, it is clear that the GFDL analysis is certainly the less smooth of these two as well.

Beyond the element of the noise in the GFDL analysis, the overall pattern of $\overline{v'T'}$ in Fig. 12 is similar in the two analyses. Indeed, in June the quantitative agreement between the major features of the GFDL and station analyses is very good. In January, there is at least one area of substantive

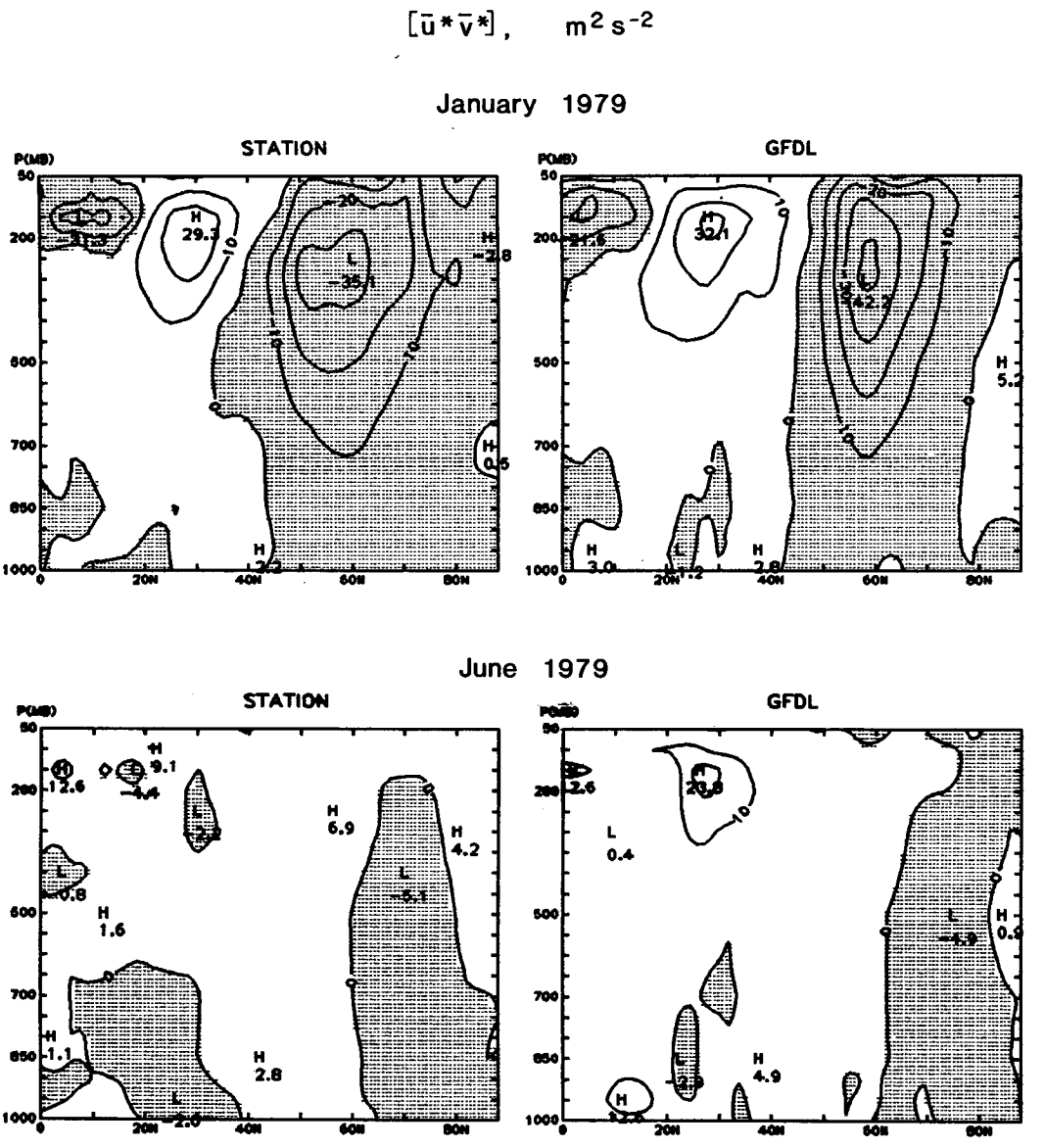

FIG. 10. Cross sections of the stationary eddy flux of momentum for January and June 1979 based on the station and the GFDL level III-b analyses. Negative values are shaded and indicate southward fluxes.

disagreement, namely in the north Pacific near the dateline.

c. Transient eddy energies and the energy cycle

In Figs. 13 and 14, we present fields that provide measures of the transient eddy kinetic and available potential energies during January. Both analyses capture the peak in the kinetic energy field at 200 mb over the North Atlantic quite well, although the GFDL analysis contains stronger gradients in the vicinity of this peak. Over the North Pacific, the station analysis, dependent largely on data from a single ocean weather ship (ship P), yields lower kinetic energies. The maxima in the 850 mb temperature variance field lie mainly over the station-rich continents. Therefore, the two fields in Fig. 14 resemble each other fairly well, although the GFDL analysis contains somewhat more intense centers and is more noisy.

The FGGE data sets offer an opportunity for a comprehensive study of the atmosphere's energy cycle. Some of this work has already begun (Kung and Tanaka, 1983, and Chen and Buja, 1983, for example). Here, our focus is simply on the differences in the energy cycle between the traditional station and GFDL level III-b analyses. For this purpose, we consider only those terms in the cycle that are easy to compute with the zonal mean quantities already in hand and

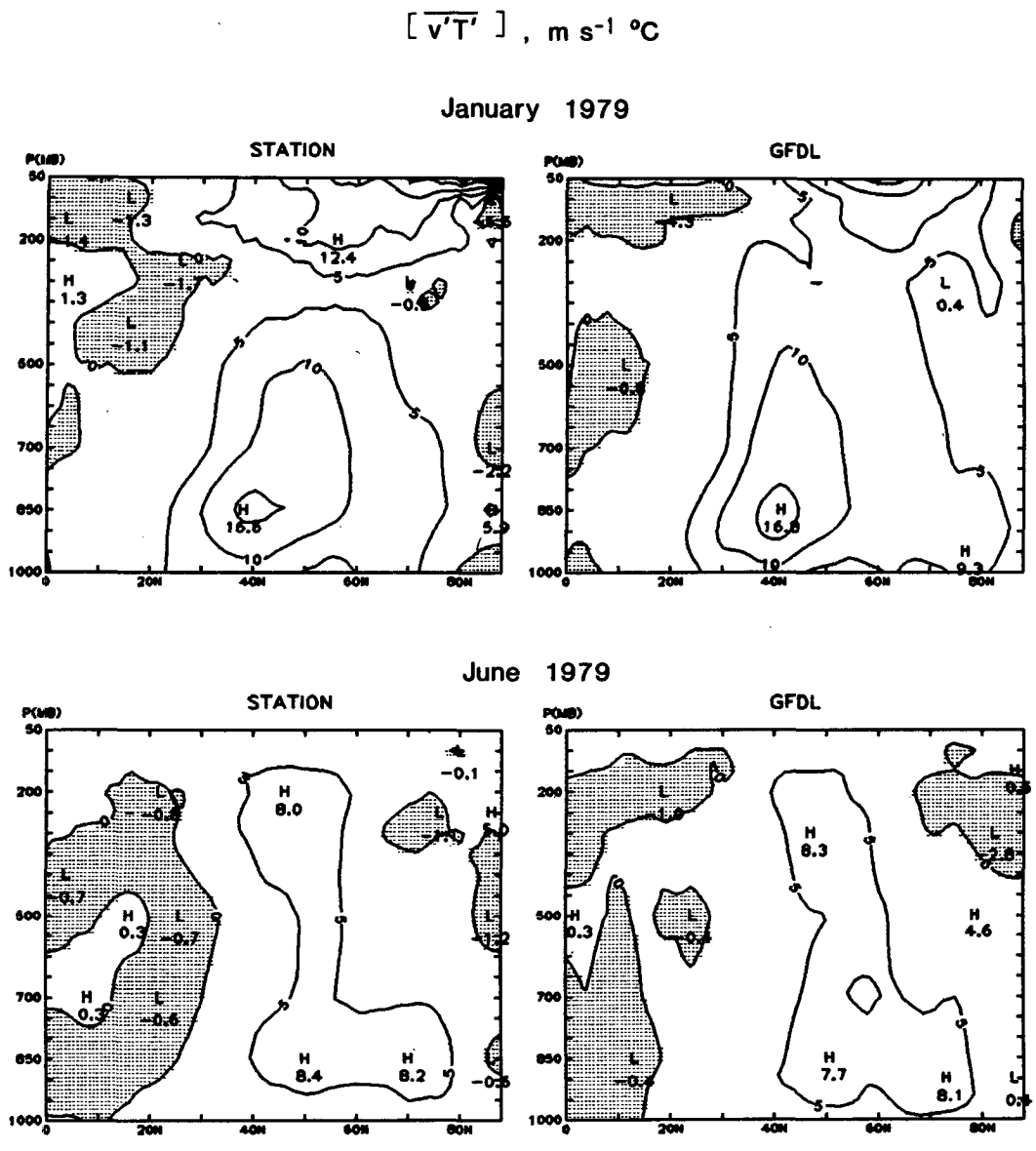

FIG. 11. Cross sections of the transient eddy flux of heat for January and June 1979 based on the station and the GFDL level III-b analyses. Negative values are shaded and indicate southward fluxes.

use the following conventional approximations to the various terms involved:

$$K_M = \frac{1}{2}\int ([\bar{u}]^2 + [\bar{v}]^2)dm,$$

where $dm = 2\pi a^2 g^{-1} \cos\phi d\phi dp$;

$$K_{TE} = \frac{1}{2}\int ([\overline{u'^2}] + [\overline{v'^2}])dm;$$

$$K_{SE} = \frac{1}{2}\int ([\bar{u}^{*2}] + [\bar{v}^{*2}])dm; \quad K_E = K_{TE} + K_{SE};$$

$$P_M = \frac{1}{2} c_p \int \gamma([\bar{T}]'')^2 dm,$$

where $[\bar{T}]'' = [\bar{T}] - \int_0^{\pi/2} [\bar{T}]\cos\phi d\phi$;

$$P_{TE} = \frac{1}{2} c_p \int \gamma[\overline{T'^2}]dm; \quad P_{SE} = \frac{1}{2} c_p \int \gamma[\bar{T}^{*2}]dm;$$

$$P_E = P_{TE} + P_{SE};$$

$$C(K_E, K_M) = \int ([\overline{u'v'}]\cos\phi + [\bar{u}^*\bar{v}^*]\cos\phi) \times \frac{\partial}{\partial\phi}\left(\frac{[\bar{u}]}{a\cos\phi}\right)dm = C(K_{TE}, K_M) + C(K_{SE}, K_M);$$

$$C(P_M, P_E) = -\int (\gamma c_p[\overline{v'T'}] + \gamma c_p[\bar{v}^*\bar{T}^*]) \times \frac{\partial}{a\partial\phi}[\bar{T}]dm = C(P_M, P_{TE}) + C(P_M, P_{SE});$$

$$C(P_M, K_M) = \int f[\bar{u}][\bar{v}]dm, \quad \text{where } f = 2\Omega\sin\phi.$$

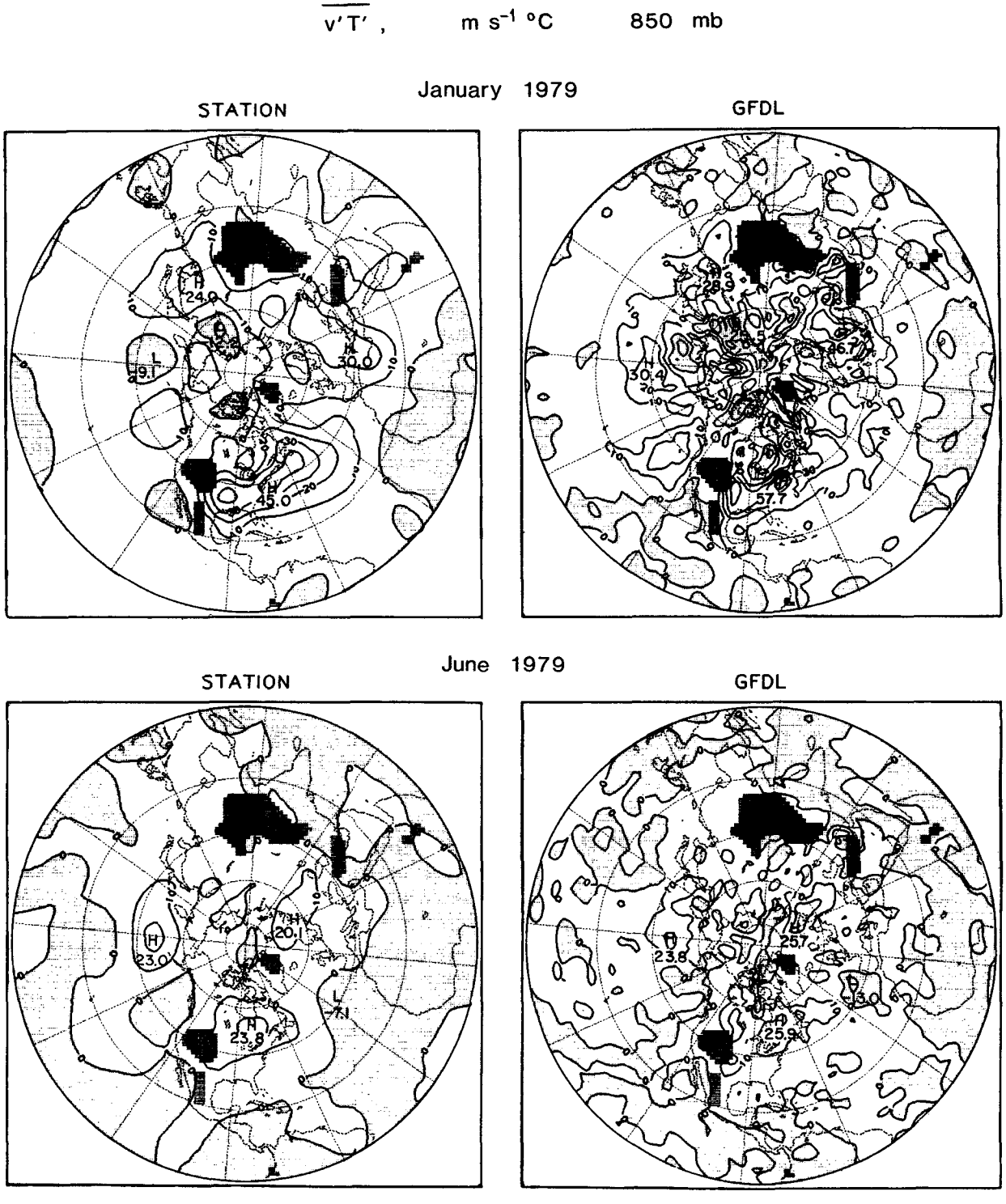

FIG. 12. Hemispheric maps of the transient eddy flux of heat at 850 mb for January and June 1979 based on the station and the GFDL level III-b analyses. Isolines are drawn at intervals of 10 m s^{-1} °C. Negative values are shaded and indicate southward fluxes. Regions where the topography is at pressures less than 850 mb are indicated by the heavy shading.

In the above, K refers to kinetic energy, in either its zonal mean (subscript M), transient eddy (TE) or stationary eddy (SE) form. Similarly, P denotes available potential energy in one of its forms. The conversion from energy form A to form B is symbolized by C(A, B). Also, c_p is the specific heat of air at constant pressure, and γ a factor related to the static stability which was calculated from the $[\bar{T}]$ fields

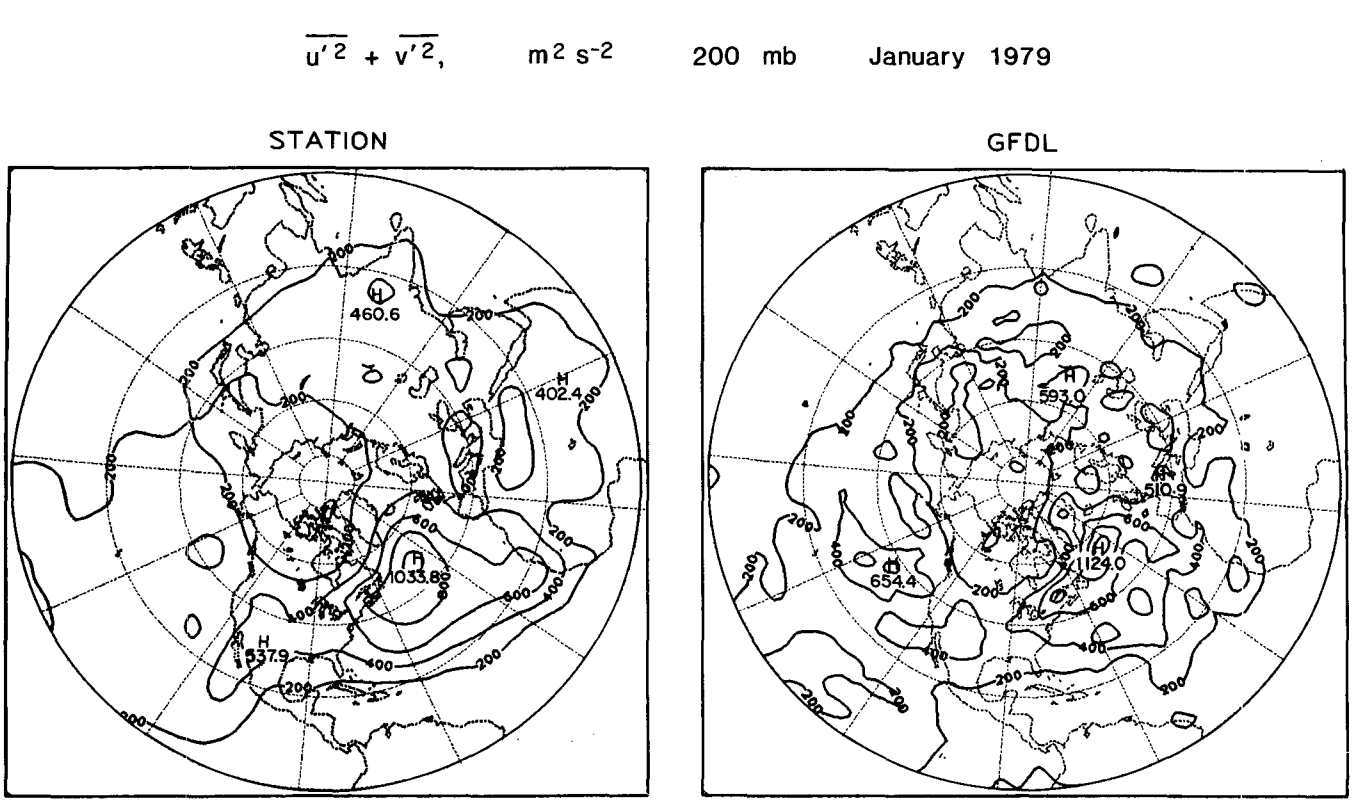

FIG. 13. Hemispheric maps of the transient eddy variance of the wind at 200 mb for January 1979 based on the station and the GFDL level III-b analyses. Isolines are drawn at intervals of 200 $m^2 s^{-2}$.

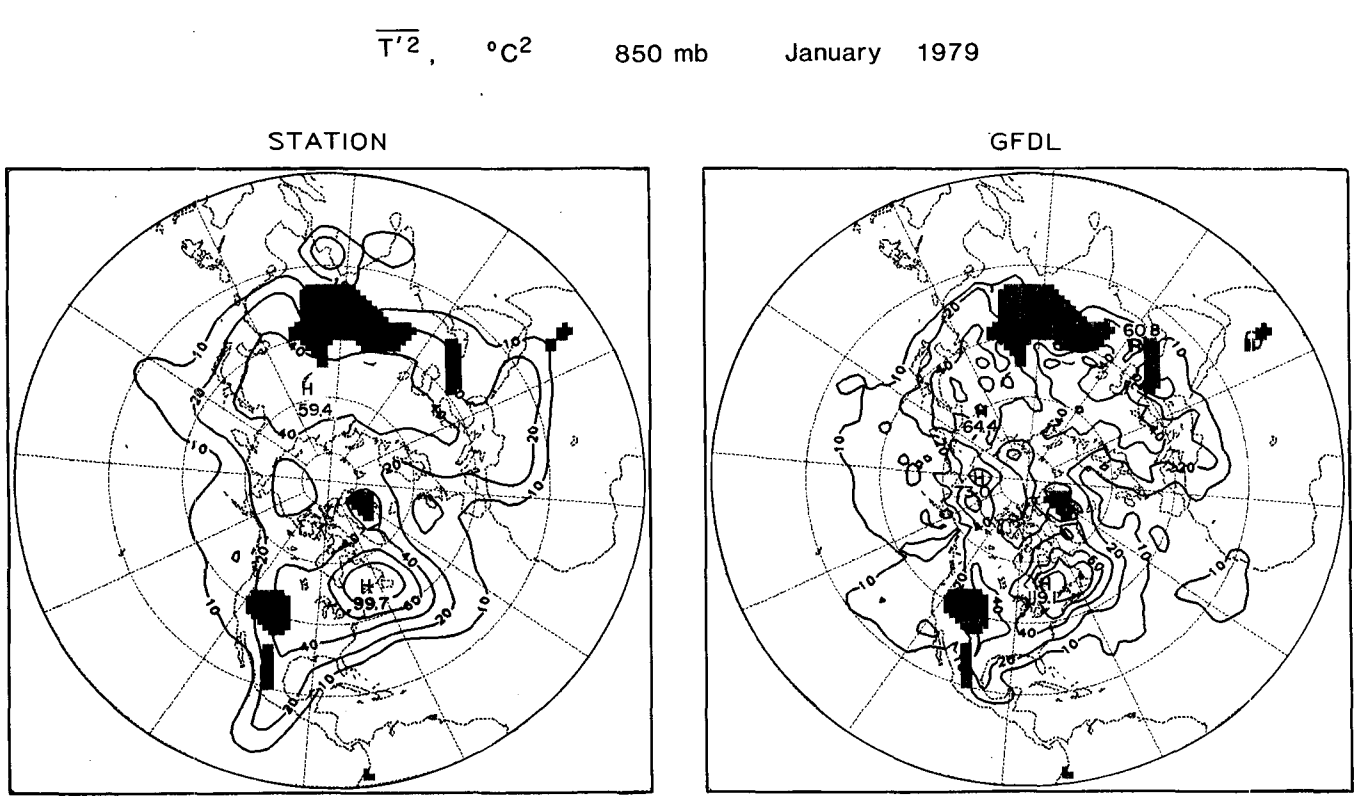

FIG. 14. Hemispheric maps of the transient eddy variance of temperature at 850 mb for January 1979 based on the station and the GFDL level III-b analyses. Isolines are generally drawn at intervals of 20 $°C^2$; a 10 $°C^2$ line is also included. Regions where the topography is at pressures less than 850 mb are indicated by the heavy shading.

separately for January and June. The limits of integration extend in latitude from equator to north pole and in pressure from 100 to 1000 mb.

Although the above equations for the energy conversions are not complete (cf. Peixoto and Oort, 1974), they do include the major components. The portions of the energy cycle calculated here are indicated by the schematic in the center of Fig. 15. By and large, the hemispheric integrals presented agree well. For example, K_{TE} in January differs only slightly between the analyses. This may seem surprising in light of the discussion above of regions at 200 mb where the station analysis produced locally smaller values. Clearly, though, these regions do not dominate when K_{TE} is integrated through the entire NH troposphere.

Two notable differences between the station and GFDL values in Fig. 15 do exist, however. The first of these is in $C(P_M, K_M)$ in both January and June. This term has proven difficult to measure accurately in the past because of its sensitivity to $[\bar{v}]$, and it appears that the FGGE year is no exception. The second difference is in $C(K_{TE}, K_M)$ in January, when the GFDL analysis actually yields a negative value for this barotropic conversion term. A review of Fig. 8 for $[\overline{u'v'}]$ and Fig. 2 for $[\bar{u}]$ reveals that this negative value results in large measure from the anomalously strong downgradient flux in the GFDL tropical upper atmosphere.

5. Water vapor and vapor fluxes

The importance of water vapor in the atmosphere, ranging from its role in the hydrological cycle to its impact on energetics, is well recognized. Despite this, measurements of water vapor in the troposphere remain relatively poor in both quality and spatial distribution. The FGGE saw no real improvement in this situation, since the satellite data available did not provide vertical profiles of water vapor. Therefore, the upper-level water vapor observations used in the GFDL level III-b analyses are drawn almost entirely from the same station data used to construct our station analyses, the aircraft dropwinsonde data being the only important difference. This commonality in the observational data base should be borne in mind when viewing the results from the two analyses.

The field of monthly mean specific humidity $\bar{q}$ at 850 mb for June is presented in Fig. 16 for both the station and GFDL analyses and for their difference. Our station analysis of the moisture fields is based on the zonal initial guess approach. The GFDL analysis is, once again, noticeably noisier, containing more detailed structure over both land and ocean. Some of the largest individual differences between the analyses exist around Pakistan and over the Arabian peninsula; however, the most widespread areas of disagreement are found over the oceans, where there was little information regarding q available

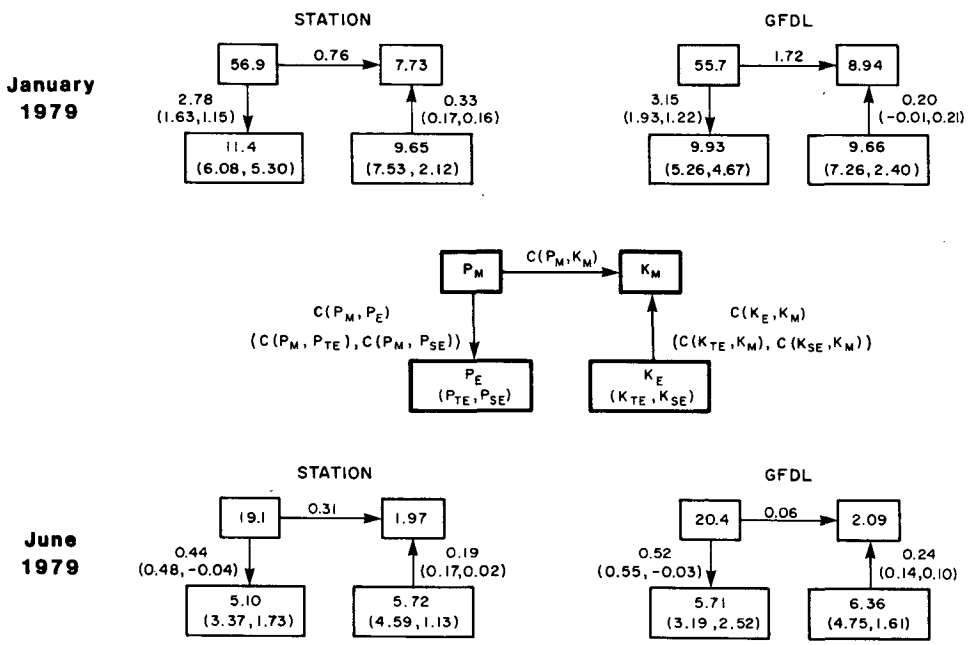

FIG. 15. Energy cycle diagrams containing values for those terms calculated in this study based on the station and the GFDL level III-b analyses for January and June 1979. Values are for the Northern Hemisphere mass between 1000 and 100 mb. The schematic in the center indicates the layout of the diagrams. Symbols are defined in the text and conversions proceed in the direction indicated by the arrows. Units for energies are 10^5 J m^{-2} and for conversions W m^{-2}.

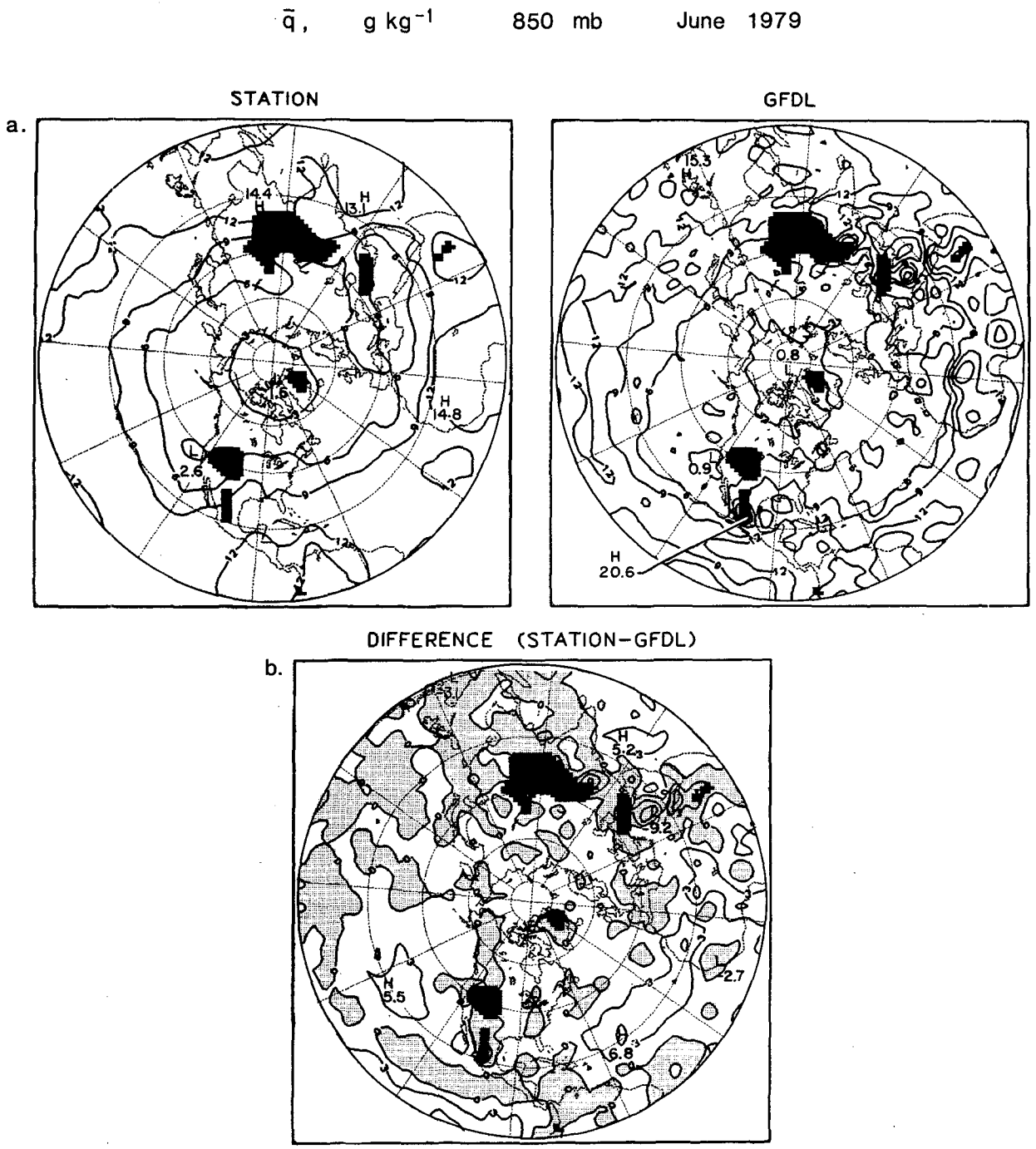

FIG. 16. (a) Hemispheric maps of the specific humidity at 850 mb for June 1979 based on the station and the GFDL level III-b analyses. Isolines are drawn at intervals of 3 g kg^{-1}. Regions where the topography is at pressures less than 850 mb are indicated by the heavy shading. (b) Difference, station analysis minus GFDL analysis, of the two fields in part (a). Isolines are drawn at intervals of 3 g kg^{-1}. Negative values are shaded and indicate higher values of specific humidity in the GFDL analysis.

to either analysis. Nevertheless, it is surprising to see differences of a factor of two in $\bar{q}$ over portions of the subtropical Atlantic, for example.

Larger values of the transient eddy flux of moisture $\overline{q'v'}$ are typically found in January than in June. Only the 850 mb fields for June 1979 are presented in Fig. 17 to illustrate a point concerning the quality control of the FGGE water vapor data. We note the extraordinarily large value for the flux over the Arabian peninsula in the GFDL analysis. This unlikely feature

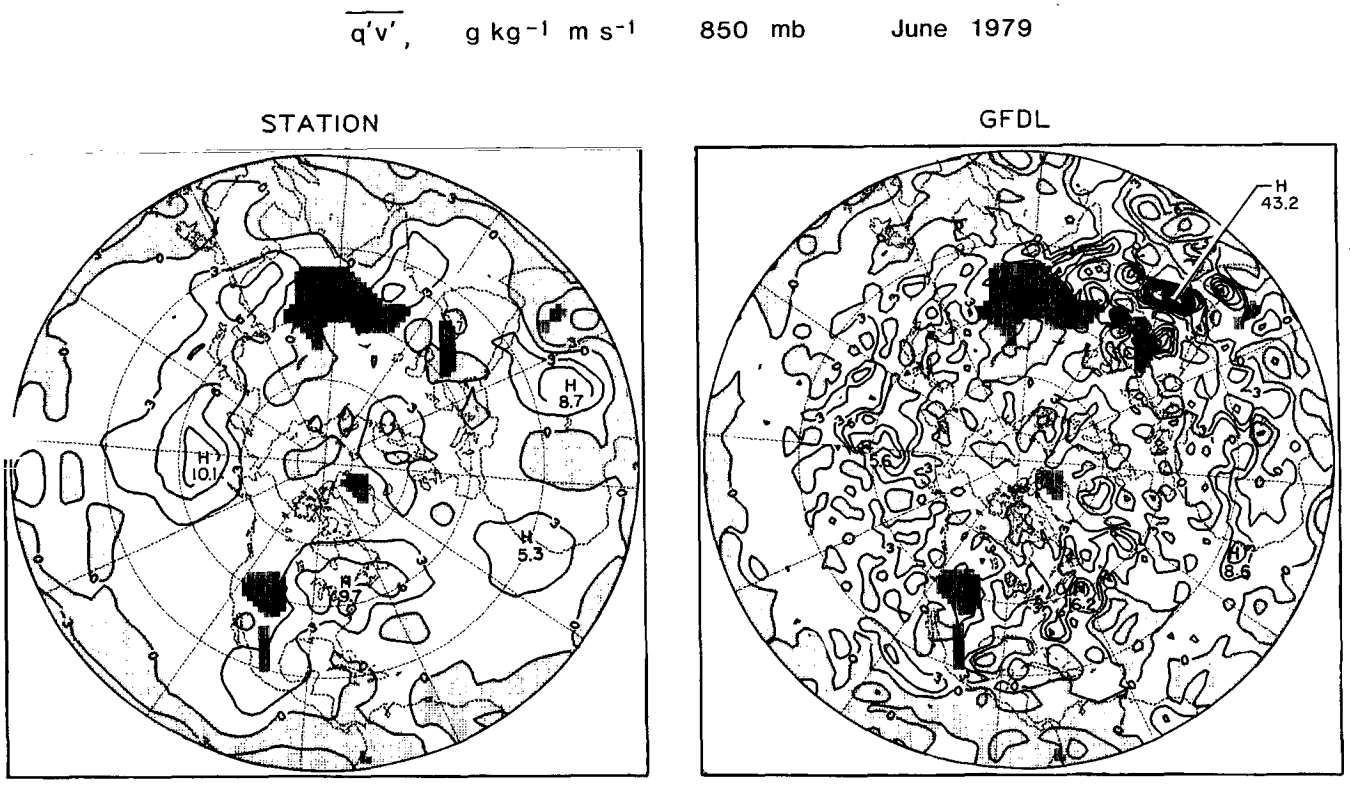

FIG. 17. Hemispheric maps of the transient eddy flux of moisture at 850 mb for June 1979 based on the station and the GFDL level III-b analyses. Isolines are drawn at intervals of 3 g kg^{-1} m s^{-1}. Negative values are shaded and indicate southward fluxes. Regions where the topography is at pressures less than 850 mb are indicated by the heavy shading.

can be traced to erratic soundings that month from station 40438 (Riyadh at 24.7°N, 46.7°E), which was eliminated from our station analysis. Elsewhere, the two analyses are in fairly close agreement with regard to the major features in $\overline{q'v'}$, although the GFDL analysis tends to produce larger values and is also, obviously, too noisy.

6. Summary and concluding remarks

We have compared a number of Northern Hemisphere (NH) circulation statistics derived for the months of January and June 1979 from FGGE level III-b analyses and from more traditional analyses based solely on the rawinsonde station data. As a result of these comparisons, the questions raised in the Introduction can at least be partially answered. With regard to zonal mean statistics and hemispheric integrals, the station network appears to yield reasonable values, over which the level III-b analyses offer little obvious improvement. The station-based zonal means are not especially sensitive to the initial guess used to generate them, and they generally agree well with the level III-b results. In the case of $[\overline{u'v'}]$, where differences of 30% do exist in the maxima between the station and GFDL analyses, the station values are supported by the ECMWF level III-b analysis. Spurious net flows of mass across latitude walls are of comparable magnitude in the station and level III-b analyses. As for the sensitive calculation of the intensity of the NH Hadley cell, the station analyses yield values that lie between those of the GFDL and ECMWF III-b analyses.

On regional scales, where the potential existed for the level III-b analyses to capture features missed by the station network, large differences between these analyses and the station-based ones do sometimes occur over station-sparse areas. Two examples described above illustrate, however, that the level III-b analyses do not necessarily provide definitive values in these areas, either. First, in the case of $\overline{u'v'}$ over the Pacific between Hawaii and the west coast of the United States, the GFDL analysis in January yields an area of very strong flux that is missed by the station analysis. However, some evidence suggests that the large value of this flux in the level III-b analyses may partly result from model biases. The second example is provided by the analysis of $\bar{u}$ in January over the subtropical western Pacific. The station analyses appear to underestimate the strength of the jet in this region, but there are also considerable differences, amounting to as much as 10 m s^{-1}, between the two level III-b analyses there.

Certain shortcomings peculiar to the GFDL analyses have been noted, such as excessively noisy fields in some instances, and lower quality of the GFDL moisture statistics. Some of the deficiencies in the level III-b analyses may result from shortcomings in the extent or accuracy of the FGGE observations themselves, despite the tremendous efforts made to improve them. Our results also indicate that uncertainties still exist in the techniques used to assimilate asynoptic satellite and aircraft data. Hopefully, our work will help guide efforts to improve these techniques.

Although our results strictly pertain to only the two months examined here, they lead us to believe that the climatologies of zonal mean statistics based on previous upper-air station data are reasonably accurate, particularly when it is realized that the station network at one time included a number of ocean weather ships. However, with the removal of Ocean Weather Ship P from the North Pacific after the FGGE year and the possible demise of all Atlantic weather ships in the next decade, it seems that station-based analyses will become less useful for generating zonal mean statistics. Nevertheless, statistics compiled at individual stations should continue to prove essential for regional studies or for delineating cohesive large-scale spatial features of interannual variability in the atmosphere. For the most part, though, we are in an era of transition, one in which we are becoming dependent on sophisticated data assimilation schemes to provide circulation statistics. Some of the results presented here and in other recent studies suggest, however, that further improvements in these schemes are needed before we can fully welcome this development.

Acknowledgments. We are grateful to the GFDL FGGE project group, and in particular to K. Miyakoda, W. Stern and J. Ploshay, for their assistance and helpful advice. R. Williams of WDC-A, Asheville offered valuable aid by supplying us with the level II-b data in the format we needed. N. Tripp of AER provided excellent programming support in connection with the station data, analyses and graphics presented here. N. Lau has been supported at the Geophysical Fluid Dynamics Program by NOAA Grant 04-7-022-44017. The material reported here is based upon work partly supported by the National Science Foundation under Grants ATM-8208690 and ATM-8311714.

REFERENCES

Bengtsson, L., 1983: Results of the global weather experiment. *The Results of the Global Weather Experiment,* WMO, No. 610, 1–40. [Available from World Meteorological Organization, Geneva, Switzerland, ISBN 92-63-10610-X.]

——, M. Kanamitsu, P. Kallberg and S. Uppala, 1982a: FGGE 4-dimensional data assimilation at ECMWF. *Bull. Amer. Meteor. Soc.,* **63,** 29–43.

——, ——, —— and ——, 1982b: FGGE research activities at ECMWF. *Bull. Amer. Meteor. Soc.,* **63,** 277–303.

Chen, T.-C., and L. E. Buja, 1983: A comparison study for the time variation of the atmospheric energetics between two hemispheres during the FGGE year: Annual variation and vacillation. *First Int. Conf. on Southern Hemisphere Meteorology,* Sao Jose dos Campos, Brazil, Amer. Meteor. Soc., 21–24.

Gordon, C. T., and W. F. Stern, 1982: A description of the GFDL global spectral model. *Mon. Wea. Rev.,* **110,** 625–644.

Kanamitsu, M., 1981: Some climatological and energy budget calculations using the FGGE III-b analyses during January 1979. *Dynamic Meteorology: Data Assimilation Methods,* L. Bengtsson *et al.,* Ed., Springer-Verlag, 263–318.

Kung, E. C., and H. Tanaka, 1983: Energetics analysis of the global circulation during the Special Observing Periods of FGGE. *J. Atmos. Sci.,* **40,** 2575–2592.

Lau, N.-C., 1984a: *Circulation Statistics Based on FGGE Level III-b Analyses Produced by GFDL.* NOAA Data Rep. ERL GFDL-5, 427 pp. [Available from GFDL, Princeton, NJ 08542]

——, 1984b: *A Comparison of Circulation Statistics Based on FGGE Level III-b Analyses Produced by GFDL and ECMWF for the Special Observing Periods.* NOAA Data Rep. ERL GFDL-6, 237 pp. [Available from GFDL, Princeton, NJ 08542]

——, and A. H. Oort, 1981: A comparative study of observed northern hemisphere circulation statistics based on GFDL and NMC analyses. Part I: The time-mean fields. *Mon. Wea. Rev.,* **109,** 1380–1403.

——, and ——, 1982: A comparative study of observed northern hemisphere circulation statistics based on GFDL and NMC analyses. Part II: Transient eddy statistics and the energy cycle. *Mon. Wea. Rev.,* **110,** 889–906.

Lorenc, A. C., and R. Swinbank, 1984: On the accuracy of general circulation statistics calculated from FGGE data—a comparison of results from two sets of analyses. *Quart. J. Roy. Meteor. Soc.,* **110,** 915–942.

Oort, A. H., 1964: On estimates of the atmospheric energy cycle. *Mon. Wea. Rev.,* **92,** 483–493.

——, 1978: Adequacy of the rawinsonde network for global circulation studies tested through numerical model output. *Mon. Wea. Rev.,* **106,** 174–195.

——, 1983: Global Atmospheric Circulation Statistics, 1958–1973. NOAA Prof. Pap. No. 14, 180 pp. [NTIS PB8 4 1297.7]

——, and E. M. Rasmusson, 1971: Atmospheric Circulation Statistics. NOAA Prof. Pap. No. 5, 323 pp. [NTIS COM-72-50295]

Peixoto, J. P., and A. H. Oort, 1974: The annual distribution of atmospheric energy on a planetary scale. *J. Geophys. Res.,* **79,** 2149–2159.

Rosen, R. D., 1976: The flux of mass across latitude walls in the atmosphere. *J. Geophys. Res.,* **81,** 2001–2002.

——, and D. A. Salstein, 1980: A comparison between circulation statistics computed from conventional data and NMC Hough analyses. *Mon. Wea. Rev.,* **108,** 1226–1247.

——, —— and J. P. Peixoto, 1979: Variability in the annual fields of large-scale atmospheric water vapor transport. *Mon. Wea. Rev.,* **107,** 26–37.

Starr, V. P., J. P. Peixoto and N. E. Gaut, 1970: Momentum and zonal kinetic energy balance of the atmosphere from five years of hemispheric data. *Tellus.* **22,** 251–274.

Stern, W. F., and J. J. Ploshay, 1983: An assessment of GFDL's continuous data assimilation system used for processing FGGE data. *Sixth Conf. on Numerical Weather Prediction,* Omaha, NE, Amer. Meteor. Soc., 90–95.

U.S. Navy, 1966: *Components of the 1000-mb Winds (or Surface Winds) of the Northern Hemisphere.* NAVAIR 50-1C-51, 86 pp. [Available from Naval Publications & Forms Center, Philadelphia, PA 19120, 0850-LP002-6500]